Figure 2. Comparison of protein and mRNA expression levels of various factors between low and highly metastatic gastric cancer cell lines. (A) Western blot analysis of total cell lysates shows protein expression levels of NDRG1, growth factor receptor, EMT-related proteins, Wnt/β-catenin-related proteins, and other factors in HSC-58, 58As1 and 58As9 cells. (B) Comparison of mRNA expression levels of NDRG1, E-cadherin, vimentin, Snail, MMP-1 and β-catenin in HSC-58, 58As1 and 58As9 cells by qRT-PCR analysis. (C) Immunocytochemical analysis of E-cadherin and β-catenin in HSC-58 and 58As9, using specific antibodies against E-cadherin, β-catenin and DAP1. Magnification×200. (D) Western blot analysis shows expression of β-catenin and Snail in nucleus and cytosol fraction. CREB, a nuclear marker, and α-tubulin, a cytosol marker. (E,F) Comparison of luciferase activity driven by E-cadhrin promoter and β-catenin (TopFlash) driven promoter between HSC-58 and its highly metastatic cell lines. The relative promoter activity is presented when normalized by the activity in HSC-58. *$p<0.01$.
doi:10.1371/journal.pone.0041312.g002

expression of the vimentin (*VIM*) and Snail (*SNAI1*). We next performed western blot and qRT-RCR analyses for several molecules that were modulated by NDRG1 knockdown in the microarray analysis (Figure 4B, C). These two cell lines showed much lower expression of both NDRG1 mRNA and protein compared to the As1/Mock3 cells. Enhanced expression of E-

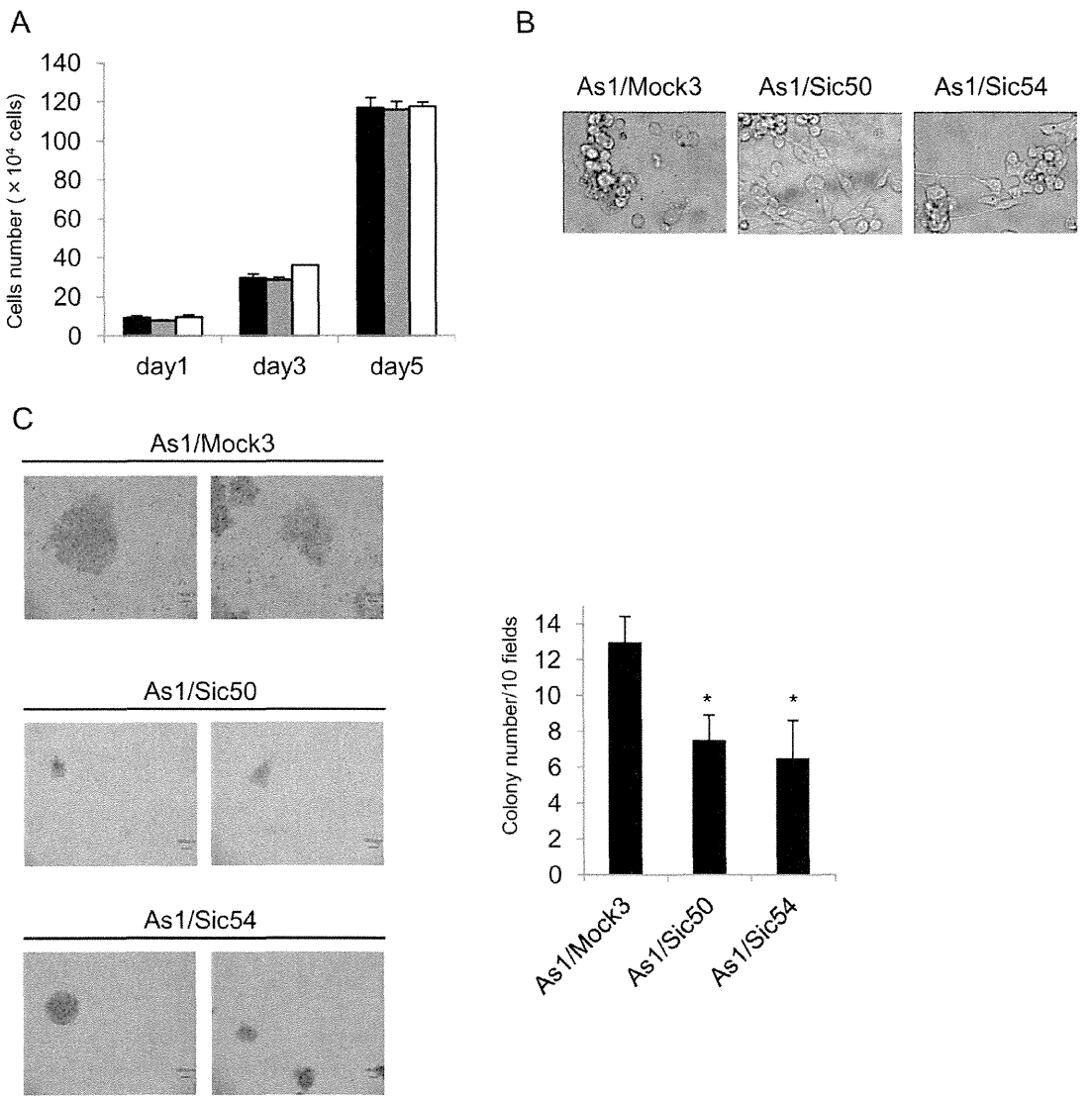

Figure 3. Comparison of biological characteristics between highly metastatic 58As1 and its NDRG1 knockdown cell lines. (A) Cell proliferation in RPMI 1640 containing 10% FBS was followed after seeding 5×10^4 cells/dish on day 0. Doubling times were similar for As1/Mock3(black), As1/Sic50(gray) and As1/Sic54(white) cells (26–30 hr). (B) Cell morphology of As1/Mock3, As1/Sic50 and As1/Sic54. Typical cell morphology in culture shows As1/Mock3 suspension-type cell growth and attached layer-type cell growth of both NDRG1 knockdowned cell lines. (C) Representative images of colonies of As1/Mock3, As1/Sic50 and As1/Sic54 when incubated for 14 days in soft agar (left panel). Quantitative analysis of colony formation activity by three cell lines when 5 dishes for each line were scored (right panel). Significant differences (*$p<0.01$) in colony number between 58As1 and its NDRG1 knockdown cell lines.
doi:10.1371/journal.pone.0041312.g003

cadherin was consistently observed in As1/Sic50 and As1/Sic54 cells compared to As1/Mock3 cells by western blot analysis. In As1/Sic50 and As1/Sic54 cells, both western blot and qRT-PCR analyses confirmed decreased expression of vimentin and Snail without affecting expression of p-ERK1/2, ERK1/2, p-Akt, Akt, p-GSK-3β and GSK-3β (Figure 4B, C).

On the other hand, NDRG1 is well known to suppress metastasis and cell proliferation by prostate and colon cancer cells. Recent studies have demonstrated that NDRG1 modulates Wnt-β-catenin signaling pathway with enhanced expression of E-cadherin in human prostate and colon cancer cell [18,19]. However, NDRG1 knockdown in 58As1 cells did not affect the β-catenin expression both at protein and mRNA level (Figure 4B, C). And also β-catenin driven promoter activity by TopFlash reporter assay revealed no difference in the promoter activity between As1/Mock and NDRG1 silenced cell lines. Therefore, β-catenin expression was not affected by NDRG1 knockdown. NDRG1 knockdown thus consistently increased expression of E-cadherin and decreased expression of Snail and vimentin in the highly metastatic cell line. However, there was no apparent change in expression of β-catenin by NDRG1 knockdown.

Enhanced E-cadherin Promoter Activity by NDRG1 Knockdown through Snail in Gastric Cancer Cells

Of various transcription factors that suppress expression of E-cadherin including Snail, Slug, Twist, TCF4 and SIP1 [20], expression of Snail was specifically modulated by NDRG1 in gastric cancer cells. We examined whether expression of E-cadherin and/or vimentin could be regulated by Snail in HSC-58 cells. Transient treatment with Snail siRNA resulted in increased expression of E-cadherin, but not that of vimentin and NDRG1, in time-dependent manner (Figure 5A). There was only a slight if any increase in β-catenin expression by Snail knockdown. Furthermore, E-cadherin promoter-driven luciferase activity was significantly suppressed by transfection of Snail complementary DNA in two cancer cell lines tested (Figure 5B). We next compared E-cadherin promoter activity between As1/Mock3 and its NDRG1 silenced cell lines. As seen in Figure 5C, there was significant ($*p<0.05$) enhancement of E-cadherin promoter activity by NDRG1 knockdown.

GSK-3β is a key enzyme for activation of EMT pathway [20,21], and also for phosphorylation of NDRG1 [22,23]. Expression of p-GSK-3β was increased in the highly metastatic cell line, 58As1 (see Figure 2A). We examined whether GSK-3β was involved in NDRG1 induced altered expression of E-cadherin and vimentin. Treatment with an inhibitor (CT99021) of GSK-3β resulted in decreased expression of p-NDRG1 and p-GSK-3β, and also increased expression of E-cadherin and β-catenin in 58As1 cells (Figure 5D). As shown in Figure 5E, β-catenin knockdown did not affect expression of E-cadherin, vimentin and Snail.

NDRG1 Knockdown Induces Mesenchymal Epithelial Transition and Suppresses Metastasis to the Peritoneum by Highly Metastatic Gastric Cancer Cells

Comparing tumor growth rates of As1/Mock3, As1/Sic50 and As1/Sic54 cells in a xenograft model revealed slower tumor growth rates of both As1/Sic50 and As1/Sic54 by NDRG1 knockdown (Figure 6A, B). NDRG1 knockdown suppressed the local invasion of As1/Mock3 tumor cells into the surrounding stroma and adjacent adipose and/or muscle tissue, and encapsulated tumor growth (Figure 6C). High expression of E-cadherin was observed in As1/Sic50 and As1/Sic54 tumors, while high expression of vimentin was observed in cancer cells of As1/Mock3 tumors (Figure 6D). By contrast, there was almost no change in expression of β-catenin in As1/Sic50 and As1/Sic54 tumors as compared with As1/Mock3 tumor.

To examine whether NDRG1 knockdown could affect metastasis to the peritoneum and accumulation of ascites, we compared the metastatic potential of As1/Sic50 and As1/Mock3 cells after orthotopic transplantation. Figure 7A shows representative images of the enlarged abdominal cavity and the presence of cancer nodules in the peritoneum. After orthotopic inoculation of As1/Sic50 cells, the number of the nodules appearing in the peritoneum was about 30% less than those resulting from As1/Mock3 cells, but this decrease was not statistically significant ($p = 0.21$) (Figure 7B). However nodules resulting from As1/Sic50 cells showed much smaller sizes than those from As1/Mock3 cells (Figure 7A). The accumulation of ascites by As1/Sic50 cells was significantly ($*p<0.01$) decreased, to about 10% of that induced by As1/Mock3 cells (Figure 7C). Furthermore, there was a significant ($*p<0.01$) increase in the survival rate of mice inoculated with As1/Sic50 cells (51±16 days) compared with 35±14 days for mice inoculated with As1/Mock3 cells, indicating that NDRG1 knockdown prolongs survival (Figure 7D).

Discussion

We have previously reported that NDRG1 is closely correlated with tumor angiogenesis and poor survival in patients with gastric cancer, suggesting that NDRG1 is a predictive biomarker for malignant progression of gastric cancer [9]. From our present study, we observed the following properties underlying the acquisition of a high metastatic potential in gastric cancer: microarray, western blot and RT-PCR analyses together revealed upregulation of NDRG1 in the highly metastatic cell lines, 58As1 and 58As9, compared with their low metastatic parental counterpart, HSC-58; higher expression of vimentin, Snail, and MMP-1, and lower expression of E-cadherin and β-catenin were evident in the highly metastatic cell lines compared with their parental counterpart; of the genes downregulated in the highly metastatic cell line, NDRG1 knockdown resulted in upregulation of E-cadherin, and downregulation of vimentin and Snail, but almost no effect on expression of β-catenin; E-cadherin promoter activity was significantly augmented by NDRG1 knockdown; NDRG1 knockdown also suppressed peritoneal dissemination and accumulation of ascites, and invasion of highly metastatic cells into surrounding normal tissues.

In the present study, NDRG1 knockdown resulted in the suppression of metastasis by highly metastatic gastric cancer cells (Figure 6, 7), suggesting that NDRG1 may be a metastasis promoter gene rather than a metastasis suppressor gene in gastric cancer. Our present study strongly supports the idea that whether NDRG1 promotes or suppresses the malignant progression of human cancer depends upon tumor types and/or differentiation status [11,12]. However, it remains unclear why NDRG1 functions as tumor suppressor or promoter depending upon tumor types or histological types. Our previous study demonstrated that NDRG1 suppresses tumor growth and angiogenesis of pancreas cancer through NDRG1 driven attenuation of NF-κB signaling pathway [24,25]. Recent study has reported that expression of metastasis suppressor gene, *KAI1* gene, is involved in NDRG1 mediated metastasis suppression of prostate cancer through ΔTF3-NF-κB pathway [26]. Further study is required to understand which regulatory mechanism is specifically responsible for NDRG1 driven promotion of malignant progression by gastric cancer cells.

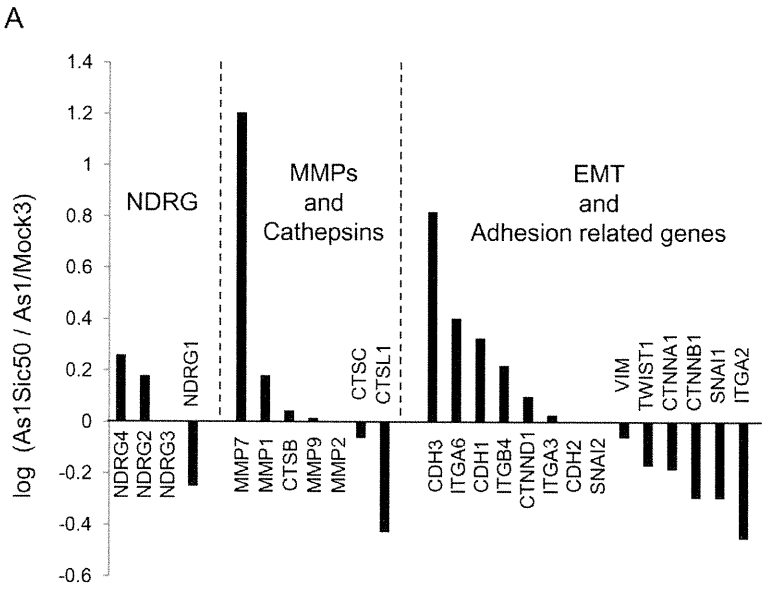
A
log (As1Sic50 / As1/Mock3)
NDRG
MMPs and Cathepsins
EMT and Adhesion related genes
NDRG4
NDRG2
NDRG3
NDRG1
MMP7
MMP1
CTSB
MMP9
MMP2
CTSC
CTSL1
CDH3
ITGA6
CDH1
ITGB4
CTNND1
ITGA3
CDH2
SNAI2
VIM
TWIST1
CTNNA1
CTNNB1
SNAI1
ITGA2

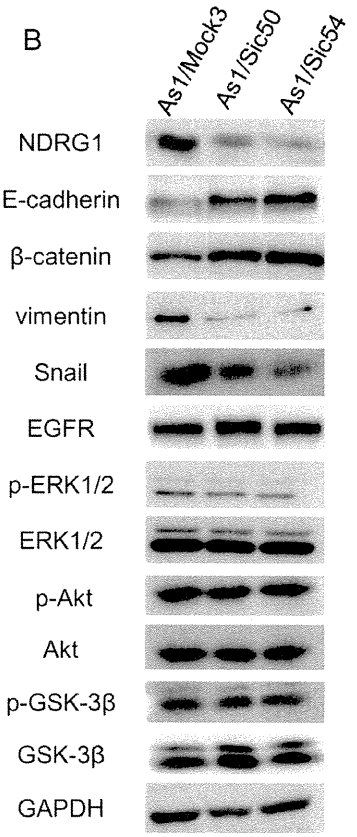
B
As1/Mock3
As1/Sic50
As1/Sic54
NDRG1
E-cadherin
β-catenin
vimentin
Snail
EGFR
p-ERK1/2
ERK1/2
p-Akt
Akt
p-GSK-3β
GSK-3β
GAPDH

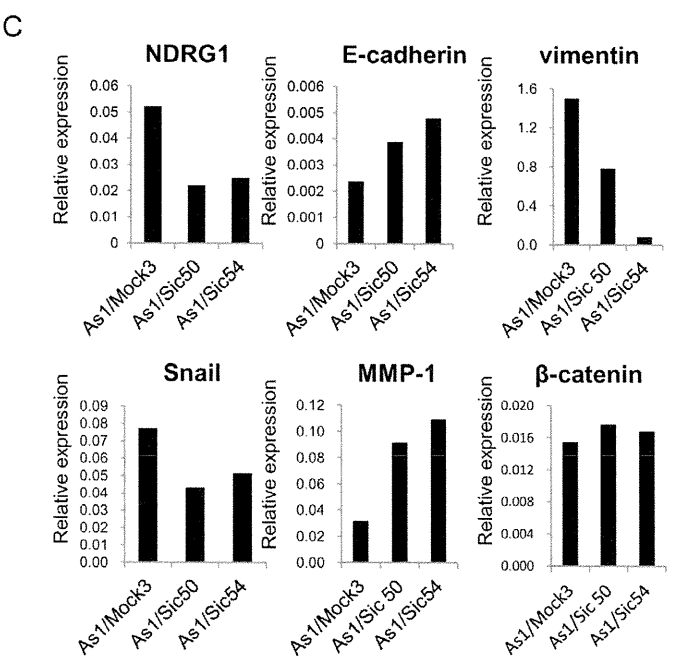
C
NDRG1
E-cadherin
vimentin
Snail
MMP-1
β-catenin
Relative expression
As1/Mock3
As1/Sic50
As1/Sic54

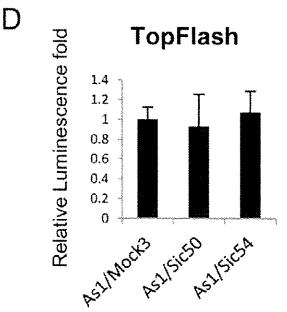
D
TopFlash
Relative Luminescence fold
As1/Mock3
As1/Sic50
As1/Sic54

Figure 4. Altered expression of EMT-related factors by NDRG1 knockdown in highly metastatic 58As1. (A) Microarray analysis for the effect of NDRG1 knockdown on expression of genes that are up- or down- regulated in AsI/Sic50 versus As1/Mock3. Relative expression rates are presented on genes belonging to three biological functions. (B) Comparison of protein expression levels of NDRG1, EMT-related proteins, β-catenin, Akt, p-Akt, ERK1/2, p-ERK1/2, GSK-3β, p-GSK-3β and EGFR by western blot analysis with total cell lysate. (C) The mRNA expression of NDRG1, E-cadherin, vimentin, Snail, MMP-1 and β-catenin was determined by qRT-PCR analysis. (D) Comparison of luciferase activity driven by β-catenin (TopFlash) between As1/Mock3 and its NDRG1 knockdowned cell lines. Relative luminescence fold is presented when normalized by the value in As1/Mock3. Each column is average of triplicate trials±SD.
doi:10.1371/journal.pone.0041312.g004

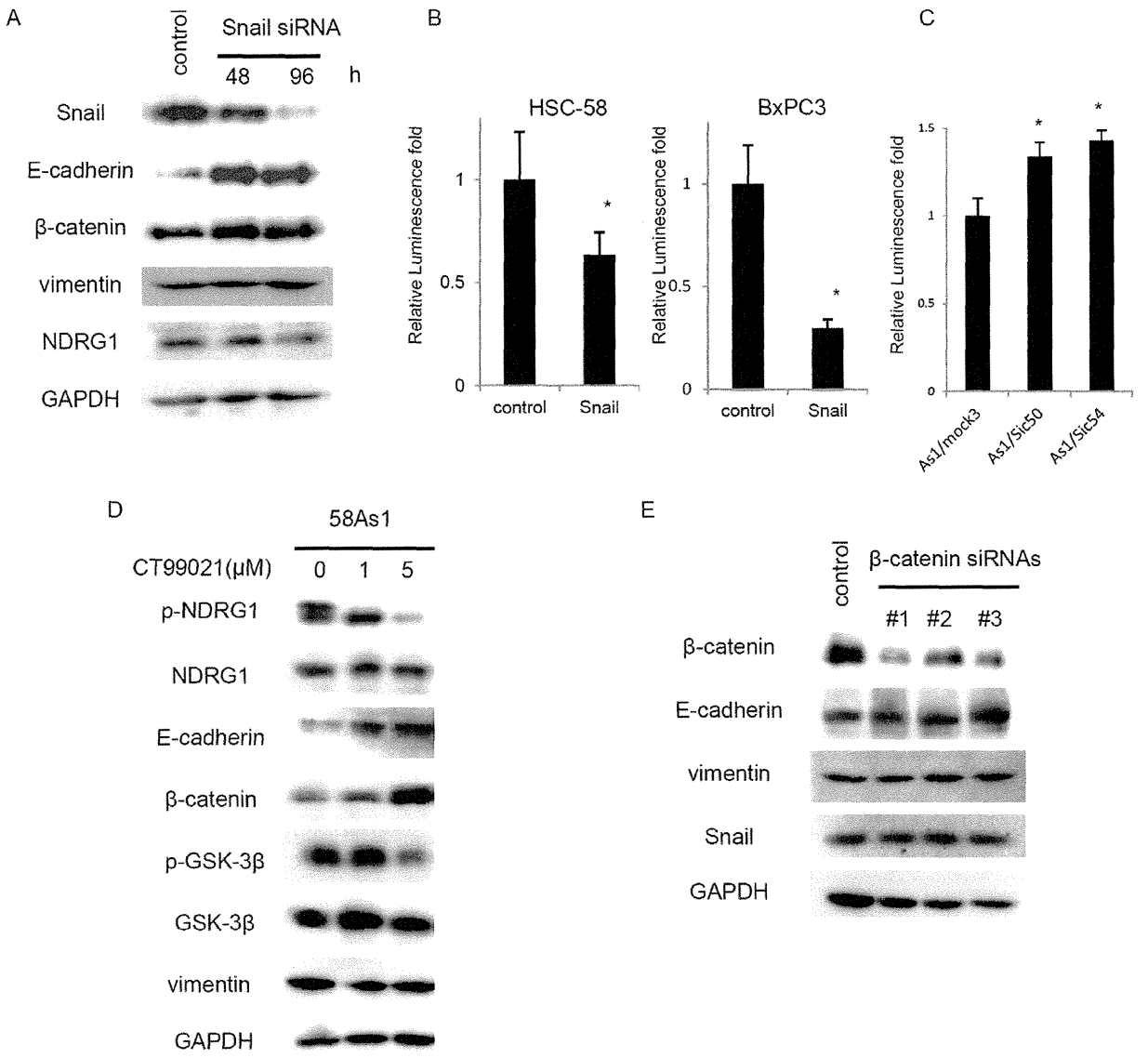

Figure 5. Enhancement of E-cadherin promoter activity by NDRG1 knockdown in highly metastatic gastric cancer cell. (A) Comparison of protein expression levels of E-cadherin, β-catenin, NDRG1 and vimentin when transiently treated with Snail siRNA for 0, 48 and 96 hr by western blot analysis in HSC-58 cell. (B) E-cadherin promoter-driven luciferase activity in the absence or presence of Snail expression in HSC-58 and BxPC-3 cells. E-cadherin-luc was transfected with or without pcDNA3-Snail, and the luciferase activity was measured. Each column is average of triplicate trials (*$p<0.05$). (C) Comparison of E-cadherin promoter-driven luciferase activity (E-cadherin-luc) in As1/Mock3, As1/Sic50 and As1/Sic54. Each column is average of triplicate trials (*$p<0.05$). (D) The effect of CT99021 on protein expression of NDRG1 and various EMT-related molecules by Western blot analysis. 58AsI cells were treated with indicated doses of the drug for 24 hr. (E) The effect of β-catenin knockdown by its siRNAs on expression of E-cadherin. HSC-58 cells were transfected with siRNAs for 24 hr, and total cell lysates were analyzed by Western blot analysis.
doi:10.1371/journal.pone.0041312.g005

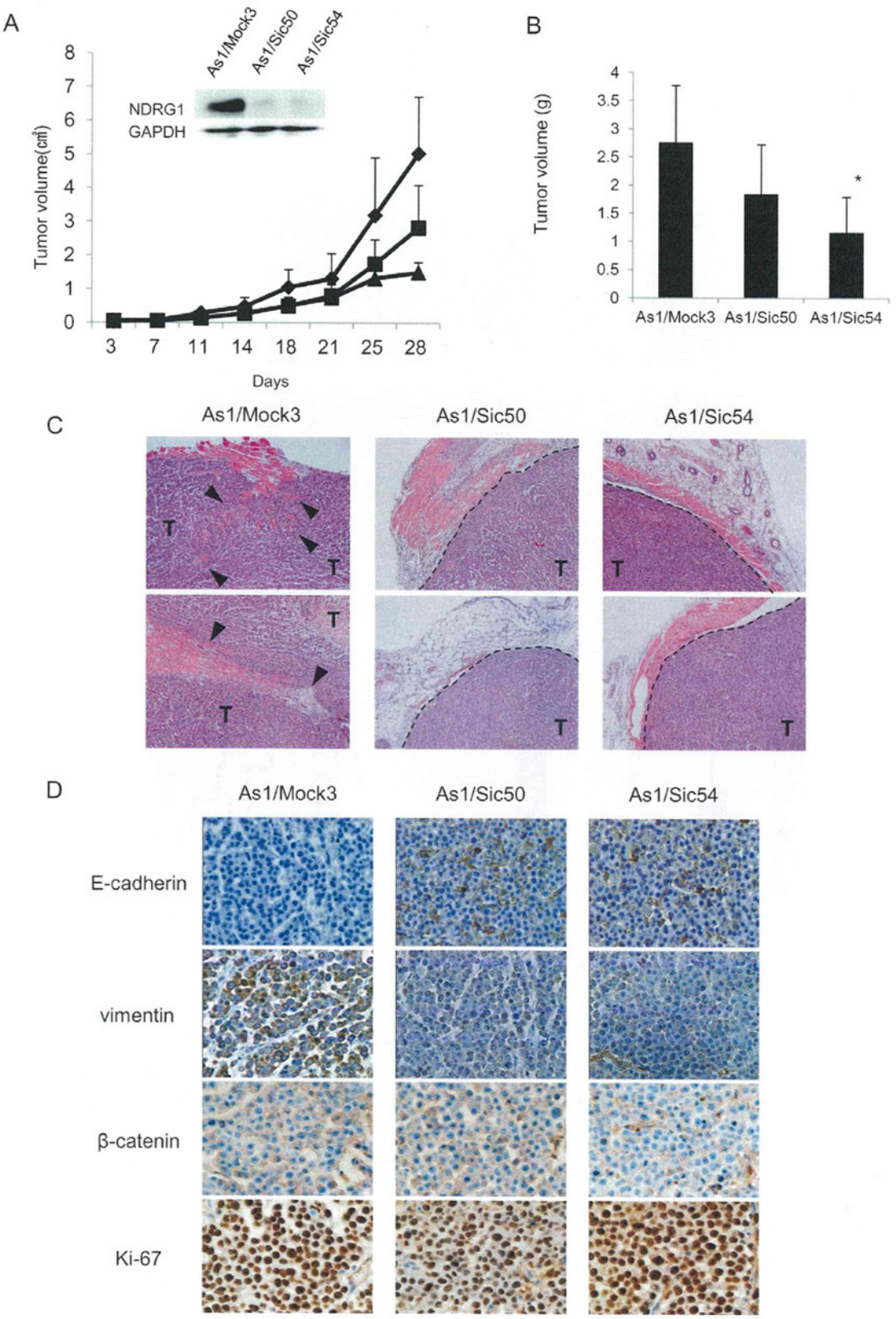
A
As1/Mock3
As1/Sic50
As1/Sic54
NDRG1
GAPDH
Tumor volume(cm³)
Days
B
Tumor volume (g)
As1/Mock3
As1/Sic50
As1/Sic54
C
As1/Mock3
As1/Sic50
As1/Sic54
T
D
As1/Mock3
As1/Sic50
As1/Sic54
E-cadherin
vimentin
β-catenin
Ki-67

Figure 6. NDRG1 knockdown suppresses tumor growth and invasion by highly metastatic cancer cell. (A) Tumor growth was followed after subcutaneous inoculation of 5×10^6 As1/Mock3 (◆), As1/Sic50 (■) and As1/Sic54 cells (▲). Inlet shows no apparent NDRG1 expression in either As1/Sic50 or As1/Sic54 tumors. (B)Tumor volume for As1/Sic50 ($p=0.87$) and As1/Sic54 cells were slightly smaller than for As1/Mock3 (day28). Each column is an average of four animals (±SD) (*$p<0.05$). (C) Representative H&E staining of tumor samples. Dashed lines indicate tumor margins, closed triangles indicate invasion of cancer cell in normal tissue. 'T' indicates tumor cells. (D) IHC images of E-cadherin, vimentin, β-catenin and Ki-67 expression in As1/Mock3, As1/Sic50 and As1/Sic54 tumors.
doi:10.1371/journal.pone.0041312.g006

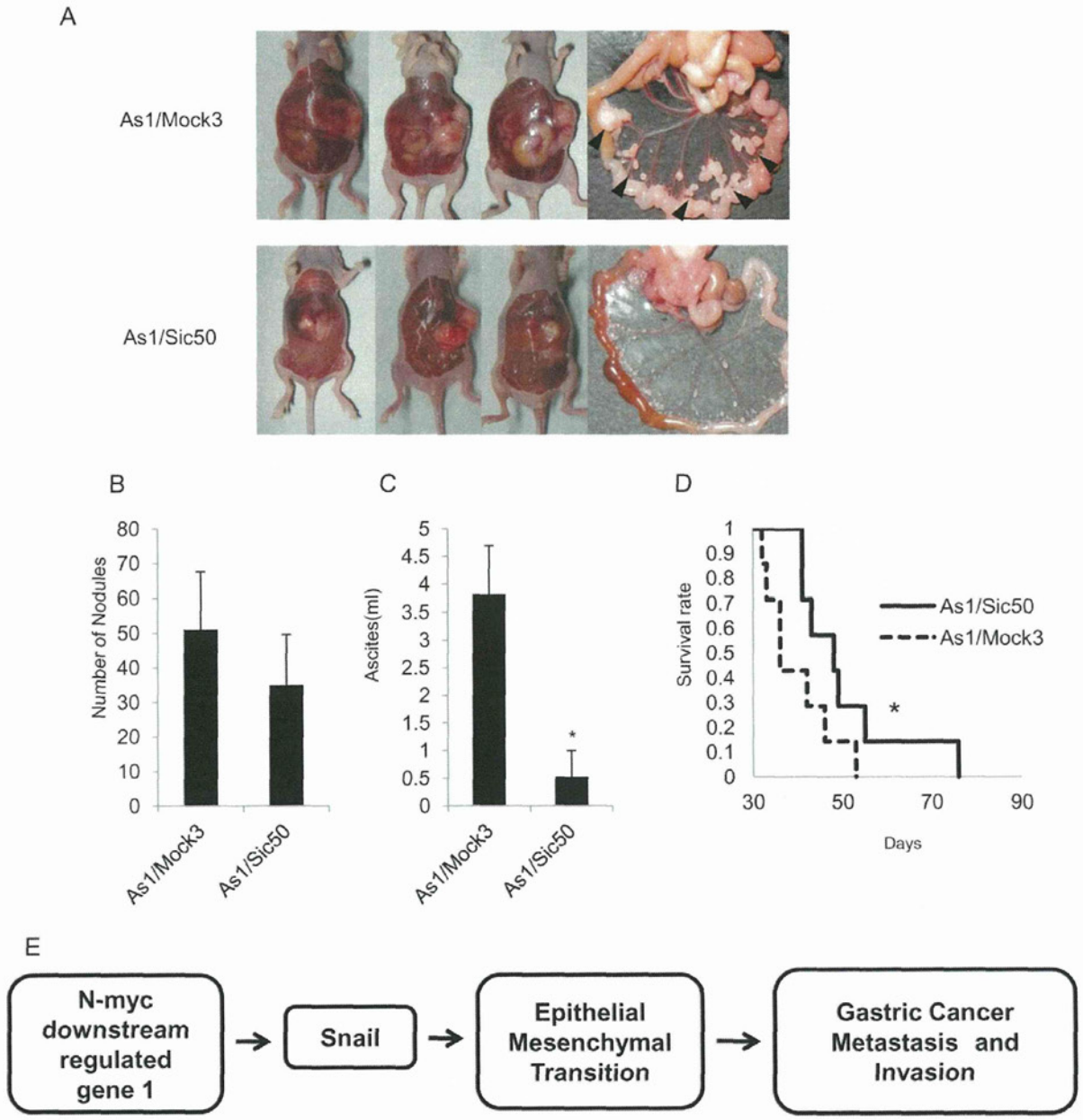

Figure 7. Suppression of peritoneal dissemination by NDRG1 knockdown. (A) Macroscopic images show enlarged peritoneal cavity and metastatic nodules by As1/Mock3 and As1/Sic50. Arrowheads show nodules. (B) Number of metastatic nodules in the mesenterium was 51±16 (As1/Mock3) and 35±14 (As1/Sic50) ($p=0.21$), but the As1/Mock3 nodule size was 3–4 times larger than those of As1/Sic50. (C) Comparison of the volume of ascites between As1/Mock3 (3.9±1.0 ml) and As1/Sic50 cells (0.5±0.6 ml) following orthotopic implantation (n = 7) (* $p<0.01$). (D) Survival curves show that survival rate in As1/Sic50 tumor-bearing mice was significantly (* $p<0.01$) longer than that of As1/Mock3 tumor-bearing mice (n = 6). (E) Our hypothetic model how NDRG1 overexpression promotes metastasis including peritoneal dissemination through alteration of EMT by scirrhous gastric cancer cells, possibly through modification of Snail expression.
doi:10.1371/journal.pone.0041312.g007

EMT is a recent highlight that could be closely associated with cancer malignant progression including acquirement of highly metastatic potential [15,16]. In our present study, NDRG1 knockdown enhanced the expression of E-cadherin and suppressed the expression of vimentin both *in vitro* and *in vivo*. NDRG1 may play a key role in the switch from a polarized epithelial phenotype to a highly motile mesenchymal phenotype. Partial or complete loss of E-cadherin is often observed during the progression toward malignancy in numerous tumors, including gastric cancer [27,28]. Oliveira et al. [29] reported a close link between E-cadherin loss and high metastatic potential in gastric cancer. Chan et al. [30] also reported soluble E-cadherin as a biomarker for prolonged survival of gastric cancer patients. NDRG1 knockdown resulted in relatively higher E-cadherin expression in As1/Sic50 tumors than in As1/Mock3 tumors, suggesting that NDRG1 may specifically control the EMT possibly through the transcription factor Snail by gastric cancer cells (Figure 7E).

Wnt signaling has pivotal roles in the malignant progression and metastasis by lung and breast cancer cells [31,32], and Wnt signaling also induces EMT which involves the metastatic progression of epithelial cancer [31,33]. NDRG1 is known as a metastasis suppressor gene in prostate and colorectal cancer cell [11,12]. Liu et al [18] has reported that NDRG1 suppresses metastasis through Wnt/β-catenin signaling pathway in prostate cancer cells. A relevant study by Chen et al [19] has also demonstrated that NDRG1 modulates TGF-β-induced EMT through altered expression of β-catenin and E-cadherin in colorectal cancer cell. Our present study showed decreased expression of β-catenin in both highly metastatic cell lines compared to the parental counterpart, HSC-58. However, both western blot and qRT-PCR analyses showed no marked change in expression levels of β-catenin and also β-catenin driven promoter activity between highly metastatic 58As1 cells and its two NDRG1 silenced cell lines. It seems less likely that β-catenin plays a pivotal role in suppression of metastasis by NDRG1 knockdown in highly metastatic cancer cells.

On the other hand, GSK-3β is also known to play a role in the control of EMT [20,21], and GSK-3β is an essential enzyme for the phosphorylation of NDRG1, an excellent substate of GSK-3β [22,23]. The expression of p-GSK3β was relatively higher in the highly metastatic cell lines than their parental cell line (Figure 2B). Treatment with a potent inhibitor of GSK-3β resulted in a suppressed expression p-NDRG1, accompanied by upregulation of E-cadherin and β-catenin (Figure 5D). However, there was almost no difference in expression of GSK-3β and p-GSK-3β by NDRG1 knockdown in the highly metastatic cells (Figure 4B), suggesting that GSK-3β may not play a major role in the induction of EMT through NDRG1 in gastric cancer cells.

Snail is a representative transcription factor that controls expression of E-cadherin [20]. Of various regulatory factors that transcriptionally control E-cadherin, expression of Snail was specifically modulated by NDRG1 in gastric cancer cell lines used in this study. Snail knockdown induced upregulation of E-cadherin (Figure 5A), and exogenous tarnsfection of Snail cDNA suppressed E-cadherin promoter activity (Figure 5B).

In highly metastatic gastric cancer cell lines, expression of Snail was upregulated as compared to their low metastatic counterpart, HSC-58 (Figure 2A, B). Both NDRG1 silenced cell lines, As1/Sic50 and As1/Sic54, showed decreased expression of Snail as compared to their highly metastatic counterpart, As1/Mock3 (Figure 4B, C). Furthermore, E-cadherin promoter activity was significantly stimulated in both NDRG1 silenced cell lines as compared to their highly metastatic counterpart (Figure 5C).

In conclusion, NDRG1 knockdown induced the upregulation of E-cadherin and downregulation of vimentin and Snail, and suppressed the invasion, metastasis and accumulation of ascites by the highly metastatic gastric cancer cells. This NDRG1 mediated regulation of E-cadherin and/or vimentin expression affected epithelial mesenchymal transition of gastric cancer cells. This NDRG1 induced modification of EMT seems to be at least in part attributable to the transcriptional factor Snail. NDRG1, in its close context with EMT-related genes, might participate in the acquisition of a high metastatic potential by progressive gastric cancer cells.

Materials and Methods

Materials and Cell Lines

HSC-58 was established from human scirrhous gastric carcinomas and 58As1 and 58As9 were independently established by repeated orthotopic implantation of HSC-58 cells into the gastric wall of athymic mice as described previously [5,6]. As1/Sic50 and As1/Sic54 cells were established by the stable transfection of NDRG1 shRNA into 58As1 cells. All cell lines were maintained in RPMI-1640 medium supplemented with 10% fetal bovine serum (FBS). BxPC-3, a human pancreatic cancer cell lines, was obtained from the American Type Culture Collection (Manassas, VA). Anti-NDRG1 antibody was generated as previously described [34]. Other antibodies were purchased as follows: anti-β-actin antibody and anti-Snail antibody were from Abcam; anti β-catenin antibody, anti-β-catenin (ser 33/37), anti-β-catenin (ser 552), anti-Wnt, anti-Ki-67, anti-GSK-3β antibody, anti-EGFR antibody, anti-GAPDH antibody, anti-p-GSK-3β antibody, anti-ERK1/2 antibody anti-p-ERK1/2 antibody, anti-AKT antibody, anti-p-AKT antibody were from Cell Signaling Technology; anti-vimentin antibody was from Calbiochem; anti-E-cadherin antibody was from BD. CT99021 was purchased from Axon Medchem BV (Netherlands).

Gene Expression Microarrays

Complementary RNA was amplified, labeled, and hybridized to a 44K Agilent 60-mer oligomicroarray according to the manufacturer's instructions (Agilent Technologies). All hybridized microarray slides were scanned by an Agilent scanner. Relative hybridization intensities and background hybridization values were calculated using Agilent Feature Extraction Software. To identify up or down-regulated genes, we calculated ratios (non-log scaled fold-changes) from the normalized signal intensities of each probe for comparison between control and experimental samples. We then established criteria for regulated genes: up-regulated genes, ratio ≥2-fold; down-regulated genes, ratio ≤0.5.

Construct of NDRG1 shRNA and Establishment of NDRG1 Knockdown Cell Lines

To obtain human a U6 siRNA vector based on pcDNA3 (Invitrogen, Carlsbad, CA), the human U6 promoter (containing *Hind*III and *Bam*HI cloning sites) was amplified from human genomic DNA with the primer pair 5′-AGATCTGAATTCCC-CAGTGGAAAGACGCGCAGGC and 5′-AGATC-TAAGCTTCTCGAGGATCCCGCGTCCTTTCCACAAGA-TATATAAACCCAAG, and ligated into the *Bgl*II site of pcDNA3. The partial DNA fragments of human NDRG1 DNA were chemically synthesized and cloned into pcDNA3-hU6siRNA cleaved with *Hind*III and *Bam*HI to produce pcDNA3shNDRG1. The synthesized DNAs for pcDNA3shNDRG1 were: 5′-GATCCGCGTGAACCCTTGTGCGGAATTCAAGA-GATTCCGCACAAGGGTTCACGTTTTTTGGAAA and: 5′-

AGCTTTTCCAAAAAACGTGAACCCTTGTGCGGAATCTC-TTGAATTCCGCACAAGGGTTCACGCG. The snail cDNA was prepared as described previously [35]. Snail cDNA was ligated into the pcDNA3 (pcDNA3-Snail). Cells were transfected with pcDNA3shNDRG1 or pcDNA3-Snail using Lipofectamine 2000 (Invitrogen) following the manufacturer's protocol. Stable transfected clones were established using G418 selection.

Transfection of Small Interfering RNA

SiRNA corresponding to nucleotide sequences of Snail and β-catenin were purchased from Invitrogen (Carlsbad, CA), respectively, siRNA duplexes were tranfected using Lipofectamine RNAiMAX and Opti-MEM medium (Invitrogen) according to the manufacture's recommendation.

Luciferase Assay

To obtain E-cadherin-Luc vector, E-cadhein promoter (−262 to +120) was amplified by PCR using the following primer pairs: 5′- AGATCTTAGTGAGCCACCGGCGGGGC-3′ and 5′-AAGCTTGGCCGGGGACGCCGAGCGAGGG-3′. Underlines indicate restriction enzyme cleavage sites. The amplified fragment was ligated into the pGEM-T easy vector (Promega) and transferred to the pGL3-basic vector (Promega) in BglII and HindIII sites. E-cadherin-luc and pcDNA3-Snail were transfected using Lipofectamine LTX and Opti-MEM medium (Invitrogen) according to the manufacture's recommendation. After 24 hr, the luciferase activity was measured according to the manufacturer's instructions (Promega). Furthermore, we also examined luciferase activity driven by β-catenin using TopFlash reporter vector as described previously [18].

Soft Agar Colony Forming Assay

4×10^3 cells were plated in 1 ml of culture medium containing 0.36% (w/v) top agar layered over a basal layer of 0.72% (w/v) agar in 6-well plates and allowed to grow for 3–4 weeks. Colonies were photographed and counted in ten random fields of view at 50X magnification using light microscopy. Each experiment was done in triplicate.

Western Blot Analysis and Fractionation of Nucleus and Cytoplasm

Cells were lysed in buffer containing 50 mM Tris-HCl, 350 mM NaCl, 0.1% NP40, 5 mM EDTA, 50 mM NaF, 1 mM phenylmethylsulfonyl fluoride, 10 μg/mL aprotinin, 10 μg/mL leupeptin, and 1 mM Na3VO4. Total cell lysates were subjected to SDS-PAGE and blotted onto Immobilon membranes (Millipore Corp., Bedford, MA) as described previously [24,25]. To prepare cytosol and nuclear fraction, cells were lysed in bufferA(10 mM HEPES, pH 7.9, 10 mM KCl, 10 mM EDTA, 1 mM DTT, 0.4% IGEPAL and protease inhibitors) and incubate for 20 min on ice. After centrifugation (3 min, 5,000 rpm), supernatant was used as cytoplasmic fraction. The resulting pellets were resuspended in bufferB (20 mM HEPES, pH 7.9, 200 mM NaCl, 1 mM EDTA, 5% glycerol, 1 mM DTT and protease inhibitors) and incubated on for 2 hr with continuous agitation at 4°C. After centrifugation (5 min, 15,000 rpm), supernatant was used as nuclear fraction. Both nuclear and cytoplasmic fraction were further analyzed by western blotting.

Quantitative Real-time Polymerase Chain Reaction (qRT-PCR)

Total RNA was isolated from cell culture using ISOGEN reagent (Nippon Gene Co. Ltd., Tokyo, Japan) according to the manufacture's instructions, as described previously [24,25]. The primer pairs and probes were obtained from Applied Biosystems. The thermal cycle conditions included maintaining the reactions at 50°C for 2 min and at 95°C for 10 min, and then alternating for 40 cycles between 95°C for 15 s and 60°C for 1 min. The relative gene expression for each sample was determined using the formula 2^(−delta Ct) = 2^(Ct(GAPDH)–Ct(target)), which reflected the target gene expression normalized to GAPDH levels.

Ethics Statement

All animal experiments were approved by the Ethics of Animal Experiments Committee at Kyushu University Graduate School of Medical Sciences. All mice were purchased from Charles River Laboratories and housed in microisolator cages maintained under a 12-hr light/dark cycle. Water and food were supplied *ad libitum*. Animals were observed for signs of tumor growth, activity, feeding, and pain in accordance with the guidelines of the Harvard Medical Area Standing Committee on Animals.

Evaluation of Tumor Growth

Tumor growth rate was tested by the subcutaneous injection of 1×10^7 cells suspended in 0.2 mL RPMI1640 medium into 6-week-old female BALB/c nude mice. Mice were examined twice weekly for tumor development. The tumor mass was measured in two dimensions with calipers, and the tumor volume was calculated according to the equation $(L\times W^2)/2$ (L = length, W-wide).

Orthotopic and Peritoneal Cavity Implantation

Orthotopic implantation was performed according to Yanagihara *et al* [5]. In brief, 6-week-old female BALB/c nude mice were anesthetized by i.p. injection of 0.28 mg/g 2.2.2-tribromoethanol (Aldrich Chemical, Milwaukee, WI). A small median abdominal incision was made under anesthesia, then 1×10^6 cells in 0.05-mL volume of RPMI medium were inoculated into the middle wall of the greater curvature of the glandular portion of the stomach using a 30-gauge needle (Nipro, Tokyo, Japan). The stomach was then returned into the peritoneal cavity, and the abdominal wall and skin were closed with an AUTOCLIP applier (Becton-Dickinson, Sparks, MD). The mice were killed when moribund, and peritoneal dissemination was evaluated by counting the number of tumor nodules in the mesenterium. We also assayed for peritoneal dissemination by direct implantation into the peritoneal cavity. We injected 1×10^6 cells in 0.5-mL volume of RPMI medium into 6-week-old female BALB/c nude mice. On day 55, we calculated the number of tumor nodules on the mesentery and the volume of ascites.

Immunocytochemical Fluorescence Analysis

Cells were seeded on glass coverslips, and then fixed with precooled methanol (−30°C) for 20 min. After washing with PBS, cells were stained with E-cadherin and β-catenin antibody. The anti- E-cadherin antibody was detected with a Cy3-labeled, antimous secondary antibody (Invitrogen). The anti-β-catenin antibody was detected with a 488-labeled, anti-rabbit secondary antibody (Cell Signaling technology). The nuclei were stained with DAPI. The cells were examined with a confocal microscope.

Immunohistochemical (IHC) Analysis of Xenograft Tumors

IHC analysis of tumors in the xenograft animal model was performed as described previously [24,25] using specific antibodies against vimentin, E-cadherin, β-catenin and Ki-67.

Acknowledgments

We thank Dr. K. Watabe (Southern Illinois University, School of Medicine, Illinois, U.S.A.) for providing us β-catenin-driven promoter construct.

Author Contributions

Conceived and designed the experiments: M. Kuwano MO. Performed the experiments: HU YM KW HI AK. Analyzed the data: M. Kage HK. Contributed reagents/materials/analysis tools: TA KN KY. Wrote the paper: M. Kuwano MO.

References

1. Hattori Y, Itoh H, Uchino S, Hosokawa K, Ochiai A, et al. (1996) Immunohistochemical detection of K-sam protein in stomach cancer. Clin Cancer Res 2: 1373–1381.
2. Hasegawa S, Furukawa Y, Li M, Satoh S, Kato T, et al. (2002) Genome-wide analysis of gene expression in intestinal-type gastric cancers using a complementary DNA microarray representing 23,040 genes. Cancer Res 62: 7012–7017.
3. Jinawath N, Furukawa Y, Hasegawa S, Li M, Tsunoda T, et al. (2004) Comparison of gene-expression profiles between diffuse- and intestinal-type gastric cancers using a genome-wide cDNA microarray. Oncogene 23: 6830–6844.
4. Oue N, Hamai Y, Mitani Y, Matsumura S, Oshimo Y, et al. (2004) Gene expression profile of gastric carcinoma: identification of genes and tags potentially involved in invasion, metastasis, and carcinogenesis by serial analysis of gene expression. Cancer Res 64: 2397–2405.
5. Yanagihara K, Tanaka H, Takigahira M, Ino Y, Yamaguchi Y, et al. (2004) Establishment of two cell lines from human gastric scirrhous carcinoma that possess the potential to metastasize spontaneously in nude mice. Cancer Sci 95: 575–582.
6. Yanagihara K, Takigahira M, Tanaka H, Komatsu T, Fukumoto H, et al. (2005) Development and biological analysis of peritoneal metastasis mouse models for human scirrhous stomach cancer. Cancer Sci 96: 323–332.
7. Yanagihara K, Takigahira M, Takeshita F, Komatsu T, Nishio K, et al. (2006) A photon counting technique for quantitatively evaluating progression of peritoneal tumor dissemination. Cancer Res 66: 7532–7539.
8. Inagaki Y, Tang W, Xu HL, Guo Q, Mafune K, et al. (2009) Localization of N-myc downstream-regulated gene 1 in gastric cancer tissue. Dig Liver Dis 41: 96–103.
9. Kawahara A, Akiba J, Hattori S, Yamaguchi T, Abe H, et al. (2011) Nuclear expression of N-myc downstream regulated gene 1/Ca^{2+}-associated protein 43 is closely correlated with tumor angiogenesis and poor survival in patients with gastric cancer. Exp Ther Med 2: 471–479.
10. Azuma K, Kawahara A, Hattori S, Taira T, Tsurutani J, et al. (2012) NDRG1/Cap43/Drg-1 may predict tumor angiogenesis and poor outcome in patients with lung cancer. J Thorac Oncol, in press.
11. Melotte V, Qu X, Ongenaert M, van Criekinge W, de Bruïne AP, et al. (2010) The N-myc downstream regulated gene (NDRG) family: diverse functions, multiple applications. FASEB J 24: 4153–4166.
12. Kovacevic Z, Richardson DR (2006) The metastasis suppressor, Ndrg-1: a new ally in the fight against cancer. Carcinogenesis 27: 2355–2366.
13. Shimono A, Okuda T, Kondoh H (1999) N-myc-dependent repression of ndr1, a gene identified by direct subtraction of whole mouse embryo cDNAs between wild type and N-myc mutant. Mech Dev 83: 39–52.
14. Cho KB, Cho MK, Lee WY, Kang KW (2010) Overexpression of c-myc induces epithelial mesenchymal transition in mammary epithelial cells. Cancer Lett 293: 230–239.
15. Polyak K, Weinberg RA (2009) Transitions between epithelial and mesenchymal states: acquisition of malignant and stem cell traits. Nat Rev Cancer 9: 265–273.
16. Iwatsuki M, Mimori K, Yokobori T, Ishii H, Beppu T, et al. (2010) Epithelial-mesenchymal transition in cancer development and its clinical significance. Cancer Sci 101: 293–299.
17. Zhou RH, Kokame K, Tsukamoto Y, Yutani C, Kato H, et al. (2011) Characterization of the human NDRG gene family: a newly identified member, NDRG4, is specifically expressed in brain and heart. Genomics 73: 86–97.
18. Liu W, Xing F, Iiizumi-Gairani M, Okuda H, Watabe M, et al. (2012) N-myc downstream regulated gene 1 modulates Wnt-β-catenin signalling and pleiotropically suppresses metastasis. EMBO Mol Med 4: 93–108.
19. Chen Z, Zhang D, Yue F, Zheng M, Kovacevic Z, et al. (2012) The iron chelators Dp44mT and DFO inhibit TGF-β-induced epithelial-mesenchymal transition via up-regulation of N-myc downstream regulated gene 1 (NDRG1). J Biol Chem 287: 17016–17028.
20. Peinado H, Olmeda D, Cano A (2007) Snail, Zeb and bHLH factors in tumour progression: an alliance against the epithelial phenotype? Nat Rev Cancer 7: 415–428.
21. Bachelder RE, Yoon SO, Franci C, de Herreros AG, Mercurio AM (2005) Glycogen synthase kinase-3 is an endogenous inhibitor of Snail transcription: implications for the epithelial-mesenchymal transition. J Cell Biol 168: 29–33.
22. Murakami Y, Hosoi F, Izumi H, Maruyama Y, Ureshino H, et al. (2010) Identification of sites subjected to serine/threonine phosphorylation by SGK1 affecting N-myc downstream-regulated gene 1 (NDRG1)/Cap43-dependent suppression of angiogenic CXC chemokine expression in human pancreatic cancer cells. Biochem Biophys Res Commun 396: 376–381.
23. Murray JT, Campbell DG, Morrice N, Auld GC, Shpiro N, et al. (2004) Exploitation of KESTREL to identify NDRG family members as physiological substrates for SGK1 and GSK3. Biochem J 15: 477–488.
24. Maruyama Y, Ono M, Kawahara A, Yokoyama A, Basaki T, et al. (2006) Tumor growth suppression in pancreatic cancer by a putative metastasis suppressor gene Cap43/NDRG1/Drg-1 through modulation of angiogenesis. Cancer Res 66: 6233–6242.
25. Hosoi F, Izumi H, Kawahara A, Murakami Y, Kinoshita H, et al. (2009) N-myc downstream regulated gene 1/Cap43 suppresses tumor growth and angiogenesis of pancreatic cancer through attenuation of inhibitor of κB kinase β expression. Cancer Res 69: 4983–4991.
26. Liu W, Ilizumi-Gairani M, Okuda H, Kobayashi A, Watanabe M, et al. (2011) KAI1 gene is engaged in NDRG1 gene-mediated metastasis suppression through the ATF3-NFκB complex in human prostate cancer. J Biol Chem, 286: 18949–18959.
27. Strumane K, Berx G, Van Roy F (2004) Cadherins in cancer. Handb Exp Pharmacol 165: 69–103.
28. Berx G, van Roy F (2009) Involvement of members of the cadherin superfamily in cancer. Cold Spring Harb Perspect Biol 1: a003129. Available: http://cshperspectives.cshlp.org/content/1/6/a003129.full. Accessed 22 May, 2012.
29. Oliveira C, Senz J, Kaurah P, Pinheiro H, Sanges R, et al. (2009) Germline CDH1 deletions in hereditary diffuse gastric cancer families. Hum Mol Genet 18: 1545–1555.
30. Chan AO, Chu KM, Lam SK, Wong BC, Kwok KF, et al. (2003) Soluble E-cadherin is an independent pretherapeutic factor for long-term survival in gastric cancer. J Clin Oncol 21: 2288–2293.
31. Nguyen DX, Chiang AC, Zhang XH, Kim JY, Kris MG, et al. (2009) WNT/TCF signaling through LEF1 and HOXB9 mediates lung adenocarcinoma metastasis. Cell 138: 51–62.
32. Zhang XH, Wang Q, Gerald W, Hudis CA, Norton L, et al. (2009) Latent bone metastasis in breast cancer tied to Src-dependent survival signals. Cancer Cell 16: 67–78.
33. Vincan E, Barker N (2008) The upstream components of the Wnt signalling pathway in the dynamic EMT and MET associated with colorectal cancer progression. Clin Exp Metastasis 25: 657–663.
34. Masuda K, Ono M, Okamoto M, Morikawa W, Otsubo W, et al. (2003) Downregulation of Cap43 gene by von Hippel-Lindau tumor suppressor protein in human renal cancer cells. Int. J. Cancer 105: 803–810.
35. Aomatsu K, Arao T, Abe K, Kodama A, Sugioka K, et al. (2012) Slug is upregulated during wound healing and regulates cellular phenotypes in corneal epithelial cells. Invest Ophthalmol Vis Sci 53: 751–756.

VOLUME 30 · NUMBER 14 · MAY 10 2012

JOURNAL OF CLINICAL ONCOLOGY

ORIGINAL REPORT

Prognostic Index for Acute- and Lymphoma-Type Adult T-Cell Leukemia/Lymphoma

Hiroo Katsuya, Takeharu Yamanaka, Kenji Ishitsuka, Atae Utsunomiya, Hidenori Sasaki, Shuichi Hanada, Tetsuya Eto, Yukiyoshi Moriuchi, Yoshio Saburi, Masaharu Miyahara, Eisaburo Sueoka, Naokuni Uike, Shinichiro Yoshida, Kiyoshi Yamashita, Kunihiro Tsukasaki, Hitoshi Suzushima, Yuju Ohno, Hitoshi Matsuoka, Tatsuro Jo, Junji Suzumiya, and Kazuo Tamura

Author affiliations appear at the end of this article.

Submitted August 10, 2011; accepted February 6, 2012; published online ahead of print at www.jco.org on April 2, 2012.

Supported in part by the Clinical Research Foundation, Fukuoka, Japan.

Authors' disclosures of potential conflicts of interest and author contributions are found at the end of this article.

Corresponding author: Kenji Ishitsuka, MD, PhD, Division of Oncology, Hematology and Infectious Diseases, Department of Internal Medicine, Fukuoka University, 7-45-1 Nanakuma, Jonan, Fukuoka 814-0180, Japan; e-mail: kenjiishitsuka@fukuoka-u.ac.jp.

0732-183X/12/3014-1635/$20.00

DOI: 10.1200/JCO.2011.38.2101

ABSTRACT

Purpose
The prognosis of acute- and lymphoma-type adult T-cell leukemia/lymphoma (ATL) is poor, but there is marked diversity in survival outcomes. The aim of this study was to develop a prognostic index (PI) for acute- and lymphoma-type ATL (ATL-PI).

Patients and Methods
In a retrospective review, data from 807 patients newly diagnosed with acute- and lymphoma-type ATL between January 2000 and May 2009 were evaluated. We randomly divided subjects into training (n = 404) and validation (n = 403) samples, and developed a PI using a multivariable fractional polynomial model.

Results
Median overall survival time (MST) for the 807 patients was 7.7 months. The Ann Arbor stage (I and II *v* III and IV), performance status (0 to 1 *v* 2 to 4), and three continuous variables (age, serum albumin, and soluble interleukin-2 receptor [sIL-2R]) were identified as independent prognostic factors in the training sample. Using these variables, a prognostic model was devised to identify different levels of risk. In the validation sample, MSTs were 3.6, 7.3, and 16.2 months for patients at high, intermediate, and low risk, respectively ($P < .001$; $\chi^2 = 89.7$, 2 *df*; log-rank test). We also simplified the original ATL-PI according to dichotomizing age at 70 years, serum albumin at 3.5 g/dL, and sIL-2R at 20,000 U/mL and developed an easily calculable PI with prognostic discrimination power ($P < .001$; $\chi^2 = 74.2$, 2 *df*; log-rank test).

Conclusion
The ATL-PI is a promising new tool for identifying patients with acute- and lymphoma-type ATL at different risks.

J Clin Oncol 30:1635-1640. © 2012 by American Society of Clinical Oncology

INTRODUCTION

Adult T-cell leukemia/lymphoma (ATL) is a peripheral T-cell malignancy caused by human T-cell lymphotropic virus type I (HTLV-1).[1,2] HTLV-1 is endemic to the southwestern region of Japan, Caribbean basin, Central and South America, and western Africa. The cumulative incidence of ATL is estimated to be approximately 2.5% to 5% among HTLV-1 carriers.[3,4] Patients with ATL present with characteristic clinical features such as increased abnormal lymphocytes with cerebriform or flower-like nuclei (flower cells) in the peripheral blood, hypercalcemia, skin lesions, generalized lymphadenopathy, and hepatosplenomegaly accompanied by opportunistic infections.[1,5] A previous report by the Japan Clinical Oncology Group-Lymphoma Study Group (JCOG-LSG) identified five prognostic factors for ATL, including advanced performance status (PS), high lactic dehydrogenase (LDH), age of 40 years or older, total involved lesions, and hypercalcemia, on the basis of an analysis of 854 patients with newly diagnosed ATL registered between 1983 and 1987.[6] The JCOG-LSG then proposed four clinical subtypes: acute, lymphoma, chronic, and smoldering types. This system is known as Shimoyama classification and is based on prognostic factors and clinical features of the disease.[7] This classification is now widely used for determining therapeutic strategy. Generally, the prognosis of acute- and lymphoma-type ATL is poor, whereas that of the chronic and smoldering types is better. More than two decades have passed since the pivotal reports by JCOG-LSG, and ATL management has improved over this period. Recently, an International Consensus Meeting recommended treatment using chemotherapies

such as a vincristine, cyclophosphamide, doxorubicin, and prednisolone (VCAP) plus doxorubicin, ranimustine, and prednisolone (AMP) plus vindesine, etoposide, carboplatin, and prednisolone (VECP), which is a sequential combination chemotherapy consisting of VCAP, AMP, and VECP[8,9] with or without subsequent allogeneic hematopoietic cell transplantation (HCT) for acute- and lymphoma-type ATL, and a combination of interferon alfa and zidovudine (IFN/AZT) for acute-type ATL outside of clinical trials.[10]

However, there are diverse clinical courses and survival outcomes among patients with acute- and lymphoma-type ATL. Therefore, it is necessary to establish a prognostic index (PI) for a risk-adapted approach and to improve the quality of clinical trials. To determine prognosis in patients with acute- and lymphoma-type ATL, we elucidated prognostic factors by performing a nationwide survey of patients diagnosed during the past decade and developed a PI.

PATIENTS AND METHODS

Patients

We conducted a retrospective survey of patients with ATL diagnosed between January 1, 2000, and May 31, 2009, in Japan. The inclusion criterion for this investigation was a diagnosis of acute- and lymphoma-type ATL based on Shimoyama classification. Patients who had undergone allogeneic HCT were excluded from this analysis because there is an undetermined impact on survival using this novel intervention. All clinical data as well as the validity of diagnosis of ATL were centrally reviewed by two expert hematologists.

Clinical Data

We collected information regarding sex, age, institutional based–clinical subtype, WBC counts, neutrophil counts, lymphoid cell counts, abnormal lymphoid cell counts, hemoglobin, platelet counts, serum total protein, serum albumin, blood urea nitrogen (BUN), LDH, soluble interleukin-2 receptor (sIL-2R), presence of hypercalcemia, C-reactive protein, maximum tumor size, "B" symptoms, PS by Eastern Cooperative Oncology Group (ECOG), Ann Arbor stage, and number of lesions of involved lymph nodes, as well as the sites and number of involved extranodal lesions. We defined leukemic stage IV disease as the presence of more than 1% of abnormal lymphocytes in peripheral blood according to the definition for diagnosing acute- and lymphoma-type ATL in Shimoyama classification.[7] Overall survival (OS) was calculated from the time of diagnosis to the date of death by any cause or to the last follow-up date.

Approval of the study procedure was obtained from the ethics committee and institutional review board of the coordinating center (Fukuoka University) and at each participating center on the basis of their institutional policies.

Statistical Analysis

The data set was randomly split into either a training sample for developing a PI or a validation sample for evaluating the obtained PI. Continuous variables were not categorized a priori because categorizing a predictor would result in an inevitable loss of information.[11] We applied parametric models based on two-degree fractional polynomial (FP) functions to retain relevant variables continuous.[12] For each continuous variable X, one or two terms of the form X^p were fitted with powers, p, which were chosen from $(-2, -1, -0.5, 0, 0.5, 1, 2, \text{and } 3)$. The association of each variable with OS was evaluated using a univariable FP model, and variables showing a P value of less than .05 were considered candidate predictors. Then, the multivariable FP (MFP) procedure using backward elimination was performed. The backward elimination was based on closed testing,[12] and a P value of less than .05 was used for variable selection. A continuous PI from the final MFP model was categorized into three risk groups, with two optimal cutoff points in the continuous PI found by maximizing the log-rank statistics according to the minimal P value approach.

An explorative simplification of our continuous PI was developed, dichotomizing all the predictors a priori according to their standard cutoff points. Concordance between three risk groups from the simplified PI and those from the original PI was measured using weighted κ.

Survival curves were estimated using the Kaplan-Meier method and compared using the log-rank test. All statistical analyses were performed with SAS version 9.2 (SAS Institute, Cary, NC) with %mfp8 macro[13] and MATLAB (Mathworks, Natick, MA). All P values were reported as two-sided.

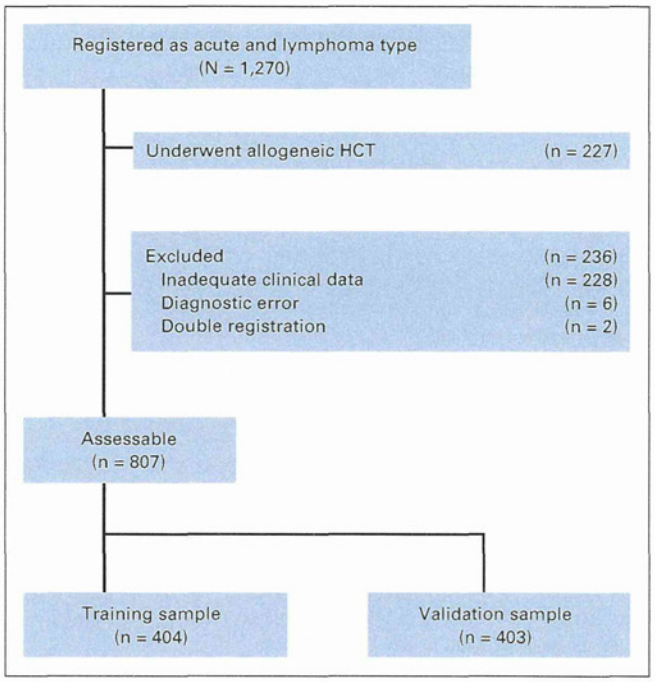

Fig 1. CONSORT flowchart of patients: 1,270 patients diagnosed with acute- and lymphoma-type adult T-cell leukemia/lymphoma were registered. Of these patients, 227 patients were excluded because they had undergone allogeneic hematopoietic cell transplantation (HCT). Two hundred thirty-six patients were excluded for the following reasons: 228 for inadequate clinical data at diagnosis because they had at least one missing value of covariates in Table 1, six for diagnostic error, and two for double registration. The remaining 807 patients were analyzed and randomly divided into training (n = 404) and validation (n = 403) samples.

RESULTS

Patient Characteristics

Data from 1,270 patients with acute- and lymphoma-type ATL were submitted from 81 institutions across Japan (Fig 1). A total of 227 patients had undergone allogeneic HCT and were excluded. Of the remaining 1,043 patients, 236 patients were excluded for the following reasons: 228 for inadequate clinical data at diagnosis because they had at least one missing value of covariates in Table 1, six for diagnostic error, and two for double registration. Thus 807 patients were analyzed for the development of the PI. Baseline characteristics are shown in Table 1. Deaths were observed in 641 patients (79%), and the median overall survival time (MST) was 7.7 months (95% CI, 7.0 to 8.7 months). The most common cause of death was progressive disease (81.3%). Death from infection without disease progression was 13.4%.

The number of patients who received initial treatment was 765 (95%), whereas 37 (4.6%) did not receive any treatment, and five were uncertain. Of the 765 patients who had received initial treatment, 755

Table 1. Baseline Characteristics of All Patients (n = 807)

Characteristic	No.	%
Age, years		
Median	67	
Range	35-91	
Sex		
Female	383	47
Male	424	53
Subtype		
Acute type	564	70
Lymphoma type	243	30
Neutrophil count, × 10^9/L		
Median	5.2	
Range	0.16-37	
Hemoglobin level, g/dL		
Median	13	
Range	7.4-18.0	
Platelet count, × 10^9/L		
Median	206	
Range	8-885	
Serum total protein, g/dL		
Median	6.6	
Range	3.2-8.9	
Serum albumin, g/dL		
Median	3.6	
Range	1.8-5.8	
BUN, mg/dL		
Median	16	
Range	3.6-118.3	
LDH, IU/L		
Median	621	
Range	127-13,813	
LDH > 2 × ULN	457	57
Soluble IL-2R, U/mL		
Median	22,800	
Range	303-683,000	
Hypercalcemia present	279	35
Increased CRP present	576	65
Ann Arbor stage		
I-II	77	10
III-IV	730	90
ECOG PS		
0-1	396	49
2-4	411	51
B symptoms present	252	31
No. of lymph node lesions		
Median	3	
Range	0-8	
No. of extranodal sites		
Median	1	
Range	0-7	
No. of total involved lesions		
Median	4	
Range	0-13	
Bone marrow involvement present	252	31
Liver involvement present	96	12
Spleen involvement present	138	17
Pleural effusion present	97	12
Ascites present	63	8

NOTE. The soluble IL-2R level by pg/mL can be converted to U/mL using the formula: value (pg/mL) × 0.113.

Abbreviations: BUN, blood urea nitrogen; CRP, C-reactive protein; ECOG PS, Eastern Cooperative Oncology Group performance status; IL-2R, interleukin-2 receptor; LDH, lactate dehydrogenase; ULN, upper limit of normal.

Table 2. Results of Variable Selection by the MFP Model in the Training Sample (n = 404)

Variable	HR	95% CI	P
Stage			
I-II	1.00		
III-IV	1.91	1.25 to 2.92	.003
ECOG PS			
0-1	1.00		
2-4	1.42	1.13 to 1.80	.003
Age, years (continuous)	1.02	1.01 to 1.03	.007
Serum albumin, g/dL (continuous)	0.70	0.57 to 0.87	.001
Log_{10}(sIL-2R), U/mL (continuous)	1.45	1.19 to 1.76	< .001

Abbreviations: ECOG PS; Eastern Cooperative Oncology Group performance status; HR, hazard ratio; MFP, multivariable fractional polynomial; sIL-2R, soluble interleukin-2 receptor.

had chemotherapy and 10 patients had undergone lesion-directed treatment (Appendix Fig A1, online only). No patient received IFN/AZT, which is considered a standard treatment for acute-type ATL in the world,[10,14] because this combination of agents has not been approved for ATL in Japan.

Development of the PI

We randomly selected 404 patients (50% of the 807 patients) as a training sample and developed a PI based on this set. First, in univariate analysis with the two-degree univariable FP model, all variables except sex showed *P* values less than .05 (likelihood ratio test). We then performed backward elimination using the MFP model. Variables that remained independently significant included Ann Arbor stage (I or II *v* III or IV), ECOG PS (0 to 1 *v* 2 to 4), and the three continuous variables of age, serum albumin, and sIL-2R. The MFP model yielded a significant nonlinear function for sIL-2R (log transformation), whereas the other four variables fitted linearly, thus allowing an expression of a final multivariate model in terms of the usual Cox regression model. The estimated hazard ratios and their 95% CIs in the final multivariate model in the training sample are shown in Table 2. A linear risk function based on Cox regression coefficients (ie, the log of hazard ratios), which hereafter we call ATL-PI, was as follows: ATL-PI = 0.65 (if stage = III or IV) + 0.35 (if ECOG PS > 1) + 0.016 × age (years) − 0.36 × albumin (g/dL) + 0.37 × $\log_{10}$ (sIL-2R [U/mL]).

The median of the ATL-PI in the training sample was 2.13 (range, 0.30 to 3.48), 10% of values were less than 1.31, and 90% of values were less than 2.86. Potential cutoff points between 1.30 and 2.90 were evaluated, and the value of 2.6 showed the best discrimination on the basis of the log-rank test (1 *df*) and was defined as the high-risk group for 91 patients (23%, ATL-PI ≥ 2.6). To define the low-risk group, the value of 1.6 was chosen as the best discriminator using the log-rank test (2 *df*), and 76 patients were classified as low risk (19%, ATL-PI < 1.6). The distribution of ATL-PI was similar in the validation sample (n = 403) with high-, intermediate-, and low-risk groups of 99 (25%), 232 (56%), and 72 (18%) patients, respectively, using the designated cutoff points. The three risk groups according to the ATL-PI were effectively prognostic in the validation sample, as shown in Figure 2 ($P < .001$; $\chi^2 = 89.7$, 2 *df*; log-rank test). MSTs were 3.6 (95% CI, 2.4 to 4.6), 7.3 (95% CI, 6.4 to 8.5), and 16.2 (95% CI, 14.5 to 24.7) months for patients at high, intermediate, and low risk, respectively, and OS rates

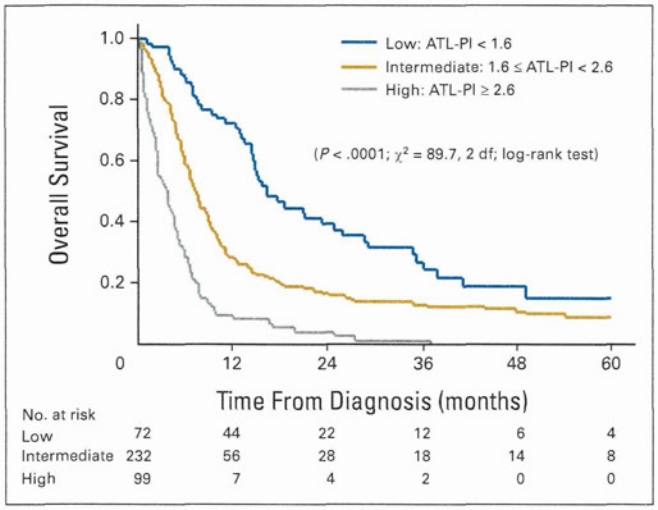

Fig 2. Overall survival curves for the validation sample (n = 403) according to the adult T-cell leukemia/lymphoma prognostic index (ATL-PI): An ATL-PI score was calculated as 0.65 (if stage = III or IV) + 0.35 (if Eastern Cooperative Oncology Group performance status > 1) + 0.016 × age (years) − 0.36 × albumin (g/dL) + 0.37 × $\log_{10}$[soluble interleukin-2 receptor (U/mL)].

Table 3. Results of Cox Regression Model With Dichotomized Covariates in the Training Sample (n = 404)

Variable	HR	95% CI	*P*	Score
Stage				
I-II	1.00			
III-IV	2.17	1.43 to 3.30	< .001	2
ECOG PS				
0-1	1.00			
2-4	1.51	1.20 to 1.90	.001	1
Age, years				
≤ 70	1.00			
> 70	1.45	1.15 to 1.83	.002	1
Serum albumin, g/dL				
≥ 3.5	1.00			
< 3.5	1.42	1.12 to 1.79	.003	1
sIL-2R, U/mL				
≤ 20,000	1.00			
> 20,000	1.37	1.09 to 1.73	.008	1

NOTE. The five variables are those selected by the multivariable fractional polynomial model. In fitting the Cox model, age, serum albumin, and sIL-2R were dichotomized. The last column shows an assigned score for each variable in the calculation of the simplified adult T-cell leukemia/lymphoma prognostic index.

Abbreviations: ECOG PS, Eastern Cooperative Oncology Group performance status; HR, hazard ratio; sIL-2R, soluble interleukin-2 receptor.

at 2 years were 4% (95% CI, 1% to 10%), 17% (95% CI, 12% to 22%), and 39% (95% CI, 27% to 51%), respectively.

Simplified ATL-PI

In the previous section, we described how a continuous PI was established from a model in which all relevant covariates were kept continuous. This PI was then used to categorize the three risk groups. Although this procedure is statistically valid for deriving the categorized risk groups,[11] to make the scoring system easier and clinically practicable, we simplified the system by initially dichotomizing individual continuous covariates. Median values of the identified continuous prognostic factors for age, serum albumin, and sIL-2R were 67 years, 3.6 g/dL, and 21,500 U/mL in the training sample, respectively. Therefore, we set the clinically appropriate cutoff points at 70 years for age, 3.5 g/dL for serum albumin, and 20,000 U/mL for sIL-2R and subsequently fitted a multivariate Cox model based on these dichotomizations in the training sample (Table 3). The estimated Cox regression coefficients were 0.77, 0.41, 0.37, 0.35, and 0.31 for the Ann Arbor stage, ECOG PS, age, albumin, and sIL-2R, respectively. From the weights of these variables, we defined a simplified ATL-PI as follows: simplified ATL-PI = 2 (if stage = III or IV) + 1 (if ECOG PS > 1) + 1 (if age > 70 years) + 1 (if albumin < 3.5 g/dL) + 1 (if sIL-2R > 20,000 U/mL).

On the basis of the best discriminations according to the log-rank test in the training sample, scores from 0 to 2 were categorized into the low-risk group, 3 and 4 into the intermediate-risk group, and from 5 to 6 into the high-risk group. The simplified ATL-PI was then applied to the validation sample, which showed a distribution from 0 through 6 (0, n = 13; 1, n = 10; 2, n = 54; 3, n = 112; 4, n = 96; 5, n = 78; 6, n = 40). Frequencies of the three risk groups were 118 patients (29%), 208 patients (52%), and 77 patients (19%), for high-, intermediate-, and low-risk groups, respectively. This classification yielded a high concordance with the original ATL-PI (weighted κ, 0.82) in the validation sample and resulted in a good separation of OS curves ($P < .001$; $\chi^2 = 74.2$, 2 *df*; log-rank test). Survival curves of the three groups according to the simplified ATL-PI are shown in Figure 3. MSTs were 4.6 (95% CI, 2.6 to 5.4), 7.0 (95% CI, 6.3 to 8.6), and 16.2 (95% CI, 13.4 to 23.2) months, and the 2-year OS rates were 6% (95% CI, 2% to 12%), 17% (95% CI, 12% to 23%), 37% (95% CI, 25% to 49%) for patients at high, intermediate, and low risk, respectively. These results indicated that the simplified ATL-PI also had good prognostic power in the validation sample.

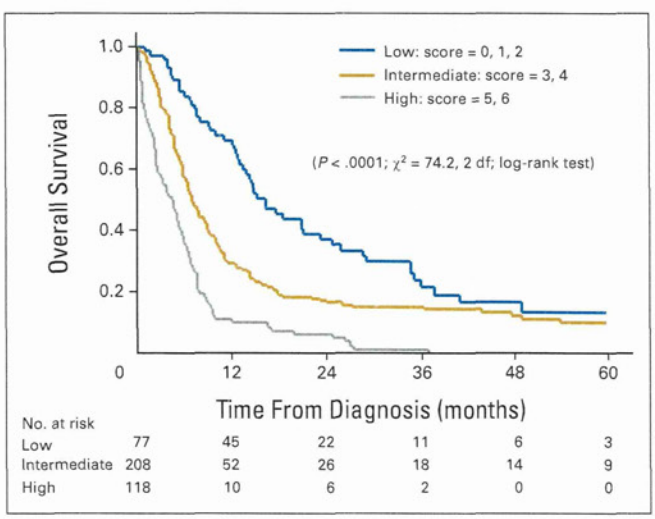

Fig 3. Overall survival curves for the validation sample (n = 403) according to the simplified adult T-cell leukemia/lymphoma prognostic index (ATL-PI): The score for the simplified ATL-PI was calculated as 2 (if stage = III or IV) + 1 (if Eastern Cooperative Oncology Group performance status > 1) + 1 (if age > 70 years) + 1 (if albumin < 3.5 g/dL) + 1 (if soluble interleukin-2 receptor > 20,000 U/mL).

Age-Adjusted ATL-PI

The simplified ATL-PI was applied to a subgroup of patients who were 60 years of age or younger (n = 109) or 70 years of age or younger (n = 255). The predictive capability of the previously determined risk factors other than age was evaluated within each age subgroup in the validation sample. Scores from 0 to 2 were categorized into the low-risk group, 3 and 4 into the intermediate-risk group, and 5 into the high-risk group. The three risk groups according to this age-adjusted ATL-PI were effectively prognostic in patient subgroups younger than 60 or 70 years of age (Appendix Fig A2, online only). MSTs were 2.8 (95% CI, 0.4 to 5.4), 6.5 (95% CI, 5.8 to 9.1), and 16.2 (95% CI, 13.4 to 35.1) months for patients at high, intermediate, and low risk among those younger than 60 years and 3.1 (95% CI, 2.1 to 5.3), 6.7 (95% CI, 5.6 to 8.4), and 16.2 (95% CI, 12.8 to 21.0) months among those younger than 70 years, respectively.

Application of ATL-PI to Patients With Allogeneic HCT

We applied the simplified ATL-PI to 192 patients with allogeneic HCT in whom data was available for five variates. The numbers of high-risk patients were as few as 12 patients (6%), whereas 97 (51%) and 83 (43%) patients showed intermediate and low risk, respectively. MSTs were 9.2 (95% CI, 4.2 to 12.7), 14.0 (95% CI, 11.0 to 17.9), and 14.3 (95% CI, 11.3 to 26.0) months at high, intermediate, and low risk, respectively (Appendix Fig A3). No statistical difference was observed among the three groups ($P = .08$; $\chi^2 = 5.04$, 2 *df*; log-rank test).

DISCUSSION

PIs for specified subentities of malignant lymphoma have involved the International Prognostic Index (IPI) for diffuse large B-cell lymphoma (DLBCL),[15] follicular lymphoma IPI for follicular lymphoma,[16] and PI for advanced Hodgkin's lymphoma.[17] PI for T-cell lymphoma, including peripheral T-cell lymphoma unspecified and extranodal natural killer T-cell lymphoma, nasal type, were also reported.[18,19] However, there have been no studies regarding PI for acute- or lymphoma-type ATL. The aim of this study was to develop a system for risk stratification in patients with acute- and lymphoma-type ATL. Importantly, this is the largest study to analyze prognosis among patients with acute- and lymphoma-type ATL, and the ATL-PI is the first PI for this cohort enabling differentiation among three subgroups with significantly different prognoses. The simplified version of the ATL-PI demonstrated a similar power of prognostic discrimination.

The ATL-PI consists of five factors: Ann Arbor stage, ECOG PS, age, serum albumin, and sIL-2R. In our multivariate analysis, the most significant factor concerning prognostic relevance to survival was the Ann Arbor stage (I or II *v* III or IV). Ann Arbor stage has been included in prognostic indices for other types of lymphoma but not emphasized in ATL because many patients with acute type fall into stage IV as a result of the leukemic phase of the disease. The prognostic significance of the Ann Arbor stage can be translated into better survival in patients with acute- and lymphoma-type ATL with limited disease. Serum sIL-2R level[20,21] was a significant novel indicator in our analyses. Notably, the survival impact of the serum sIL-2R levels was stronger than LDH levels, which are commonly included in PIs for many types of malignant lymphoma. It is thus conceivable that serum sIL-2R can be a new marker of tumor load in ATL.

Recent analysis of 126 patients from the International Peripheral T-Cell Lymphoma Project suggested that the IPI, which is commonly used in the management of patients with DLBCL,[15] is also a useful tool for predicting clinical outcome of patients with ATL.[22] However, in contrast to our study, most patients registered in the previous project had lymphoma type. We applied the IPI to 403 patients in the validation sample and confirmed that most patients were allocated into the intermediate- or high-risk groups, whereas patients in the low-risk group accounted for only 5.7%; the median age of 67 years in our analysis was higher than that in patients involved in the IPI study (56 years),[15] and many more patients with ATL than with DLBCL were in stage IV as a result of frequent leukemic manifestation in the peripheral blood. Moreover, 89% of patients surpassed the normal upper limit of LDH in our study. A similar tendency was observed in applying the PI for peripheral T-cell lymphoma unspecified to the validation sample.[18]

We additionally investigated the simplified ATL-PI according to chemotherapeutic regimens. The MSTs were 4.8, 7.3, and 14.7 months for patients with a cyclophosphamide, doxorubicin, vincristine, and prednisolone (CHOP)/CHOP-like regimen at high, intermediate, and low risk, respectively, and 5.3, 8.7, and 14.9 months for patients with VCAP-AMP-VECP, respectively. Thus the simplified ATL-PI was not affected by chemotherapeutic regimens.

We excluded patients treated with allogeneic HCT in our analysis because allogeneic HCT has an undetermined impact on survival. In fact, allogeneic HCT may have the potential to put some patients into cure, thus significantly prolonging their survival, whereas allogeneic HCT causes an observed treatment-related mortality of up to 43%,[23-25] implying that prognoses of a specific fraction of patients are perturbed by this intervention. We applied the simplified ATL-PI to patients who received allogeneic HCT, but it was not possible to distinguish patient subgroups between low and intermediate risks. This may be because transplantation was applied to a particular population who could complete induction treatment and survived until transplantation (6 months median since diagnosis), regardless of their risk classification. The predominant difference appears in the intermediate-risk group, where the MSTs were 14.0 and 6.5 months for patients with allogeneic HCT and standard therapy, respectively, suggesting that allogeneic HCT might have improved the prognosis for the group, although this should be interpreted with caution because of the potential bias in patient selection for transplant. There is a need for a larger study to address this issue.

In conclusion, we proposed an original ATL-PI and its simplified version including five prognostic factors for acute- and lymphoma-type ATL. The ATL-PI, the first PI for acute- and lymphoma-type ATL, is a promising platform that can be used to determine optimal treatment based on risk stratification and for well-controlled clinical trials. Further international studies including patients treated with IFN/AZT, which is a common treatment for acute-type ATL outside Japan, is warranted to assess the power of the ATL-PI.

AUTHORS' DISCLOSURES OF POTENTIAL CONFLICTS OF INTEREST

The author(s) indicated no potential conflicts of interest.

AUTHOR CONTRIBUTIONS

Conception and design: Takeharu Yamanaka, Kenji Ishitsuka, Junji Suzumiya, Kazuo Tamura
Collection and assembly of data: Hiroo Katsuya, Kenji Ishitsuka, Atae Utsunomiya, Hidenori Sasaki, Shuichi Hanada, Tetsuya Eto, Yukiyoshi Moriuchi, Yoshio Saburi, Masaharu Miyahara, Eisaburo Sueoka, Naokuni Uike, Shinichiro Yoshida, Kiyoshi Yamashita, Kunihiro Tsukasaki, Hitoshi Suzushima, Yuju Ohno, Hitoshi Matsuoka, Tatsuro Jo, Junji Suzumiya
Data analysis and interpretation: Hiroo Katsuya, Takeharu Yamanaka, Kenji Ishitsuka
Manuscript writing: All authors
Final approval of manuscript: All authors

REFERENCES

1. Uchiyama T, Yodoi J, Sagawa K, et al: Adult T-cell leukemia: Clinical and hematologic features of 16 cases. Blood 50:481-492, 1977
2. Poiesz BJ, Ruscetti FW, Gazdar AF, et al: Detection and isolation of type C retrovirus particles from fresh and cultured lymphocytes of a patient with cutaneous T-cell lymphoma. Proc Natl Acad Sci U S A 77:7415-7419, 1980
3. Murphy EL, Hanchard B, Figueroa JP, et al: Modelling the risk of adult T-cell leukemia/lymphoma in persons infected with human T-lymphotropic virus type I. Int J Cancer 43:250-253, 1989
4. Yamaguchi K, Watanabe T: Human T lymphotropic virus type-I and adult T-cell leukemia in Japan. Int J Hematol 76:240-245, 2002 (suppl 2)
5. Ishitsuka K, Tamura K: Treatment of adult T-cell leukemia/lymphoma: Past, present, and future. Eur J Haematol 80:185-196, 2008
6. Major prognostic factors of patients with adult T-cell leukemia-lymphoma: A cooperative study—Lymphoma Study Group (1984-1987). Leuk Res 15:81-90, 1991
7. Shimoyama M: Diagnostic criteria and classification of clinical subtypes of adult T-cell leukaemia-lymphoma: A report from the Lymphoma Study Group (1984-87). Br J Haematol 79:428-437, 1991
8. Yamada Y, Tomonaga M, Fukuda H, et al: A new G-CSF-supported combination chemotherapy, LSG15, for adult T-cell leukaemia-lymphoma: Japan Clinical Oncology Group Study 9303. Br J Haematol 113:375-382, 2001
9. Tsukasaki K, Utsunomiya A, Fukuda H, et al: VCAP-AMP-VECP compared with biweekly CHOP for adult T-cell leukemia-lymphoma: Japan Clinical Oncology Group Study JCOG9801. J Clin Oncol 25:5458-5464, 2007
10. Tsukasaki K, Hermine O, Bazarbachi A, et al: Definition, prognostic factors, treatment, and response criteria of adult T-cell leukemia-lymphoma: A proposal from an international consensus meeting. J Clin Oncol 27:453-459, 2009
11. Royston P, Altman DG, Sauerbrei W: Dichotomizing continuous predictors in multiple regression: A bad idea. Stat Med 25:127-141, 2006
12. Royston P, Sauerbrei W: Multivariable Model-building: A Pragmatic Approach to Regression Analysis Based on Fractional Polynomials for Modelling Continuous Variables. Hoboken, NJ, Wiley, 2008
13. Sauerbrei W, Meier-Hirmer C, Benner A, et al: Multivariable regression model building by using fractional polynomials: Description of SAS, STATA and R programs. Comput Stat Data Anal 50:3464-3485, 2006
14. Bazarbachi A, Plumelle Y, Carlos Ramos J, et al: Meta-analysis on the use of zidovudine and interferon-alfa in adult T-cell leukemia/lymphoma showing improved survival in the leukemic subtypes. J Clin Oncol 28:4177-4183, 2010
15. A predictive model for aggressive non-Hodgkin's lymphoma: The International Non-Hodgkin's Lymphoma Prognostic Factors Project. N Engl J Med 329:987-994, 1993
16. Solal-Céligny P, Roy P, Colombat P, et al: Follicular lymphoma international prognostic index. Blood 104:1258-1265, 2004
17. Hasenclever D, Diehl V: A prognostic score for advanced Hodgkin's disease: International Prognostic Factors Project on Advanced Hodgkin's Disease. N Engl J Med 339:1506-1514, 1998
18. Gallamini A, Stelitano C, Calvi R, et al: Peripheral T-cell lymphoma unspecified (PTCL-U): A new prognostic model from a retrospective multicentric clinical study. Blood 103:2474-2479, 2004
19. Lee J, Suh C, Park YH, et al: Extranodal natural killer T-cell lymphoma, nasal-type: A prognostic model from a retrospective multicenter study. J Clin Oncol 24:612-618, 2006
20. Kamihira S, Atogami S, Sohda H, et al: Significance of soluble interleukin-2 receptor levels for evaluation of the progression of adult T-cell leukemia. Cancer 73:2753-2758, 1994
21. Araki K, Harada K, Nakamoto K, et al: Clinical significance of serum soluble IL-2R levels in patients with adult T cell leukaemia (ATL) and HTLV-1 carriers. Clin Exp Immunol 119:259-263, 2000
22. Suzumiya J, Ohshima K, Tamura K, et al: The International Prognostic Index predicts outcome in aggressive adult T-cell leukemia/lymphoma: Analysis of 126 patients from the International Peripheral T-Cell Lymphoma Project. Ann Oncol 20:715-721, 2009
23. Kami M, Hamaki T, Miyakoshi S, et al: Allogeneic haematopoietic stem cell transplantation for the treatment of adult T-cell leukaemia/lymphoma. Br J Haematol 120:304-309, 2003
24. Fukushima T, Miyazaki Y, Honda S, et al: Allogeneic hematopoietic stem cell transplantation provides sustained long-term survival for patients with adult T-cell leukemia/lymphoma. Leukemia 19: 829-834, 2005
25. Hishizawa M, Kanda J, Utsunomiya A, et al: Transplantation of allogeneic hematopoietic stem cells for adult T-cell leukemia: A nationwide retrospective study. Blood 116:1369-1376, 2010

Affiliations

Hiroo Katsuya, Kenji Ishitsuka, Hidenori Sasaki, and Kazuo Tamura, Fukuoka University; Tetsuya Eto, Hamanomachi Hospital; Naokuni Uike, National Kyushu Cancer Center, Fukuoka; Takeharu Yamanaka, National Cancer Center Hospital East; Atae Utsunomiya, Imamura Bun-in Hospital, Kagoshima; Shuichi Hanada, National Hospital Organization Kagoshima Medical Center, Kagoshima; Yukiyoshi Moriuchi, Sasebo City General Hospital, Sasebo; Yoshio Saburi, Oita Prefectural Hospital, Oita; Masaharu Miyahara, Karatsu Red Cross Hospital, Karatsu; Eisaburo Sueoka, Saga University Hospital, Saga; Shinichiro Yoshida, National Hospital Organization Nagasaki Medical Center, Ohmura; Kiyoshi Yamashita, Miyazaki Prefectural Hospital; Hitoshi Matsuoka, Koga General Hospital, Miyazaki; Kunihiro Tsukasaki, Nagasaki University Graduate School of Biomedical Science; Tatsuro Jo, Japanese Red Cross Nagasaki Genbaku Hospital, Nagasaki; Hitoshi Suzushima, Nippon Telegraph and Telephone Corporation West Kyushu Hospital, Kumamoto; Yuju Ohno, Kitakyushu Municipal Medical Center, Kitakyushu; and Junji Suzumiya, Shimane University, Izumo, Japan.

VOLUME 31 · NUMBER 1 · JANUARY 1 2013

JOURNAL OF CLINICAL ONCOLOGY

DIAGNOSIS IN ONCOLOGY

Severe Acute Interstitial Lung Disease After Crizotinib Therapy in a Patient With *EML4-ALK*–Positive Non–Small-Cell Lung Cancer

Introduction

The development of epidermal growth factor receptor (EGFR) tyrosine kinase inhibitors (TKIs) such as erlotinib and gefitinib, and, more recently, that of the anaplastic lymphoma kinase (ALK) TKI crizotinib, has had a profound impact on the treatment of advanced non–small-cell lung cancer (NSCLC).[1-3] The occurrence of EGFR-TKI–associated interstitial lung disease (ILD) in patients with NSCLC has been found to be more frequent among Japanese patients than among white patients.[4,5]

Case Report

A 39-year-old male current-smoker (30 pack years) of Japanese descent was diagnosed with poorly differentiated stage IV lung adenocarcinoma (T4N3M1b) with multiple pleural dissemination as well as intra-abdominal lymph node and brain metastasis. Mutation analysis of biopsied tumor tissue showed that the tumor was wild type for the *EGFR* gene. Fluorescence in situ hybridization analysis with break-apart probes for the *ALK* gene revealed the presence of an *ALK* rearrangement, and subsequent reverse transcription and polymerase chain reaction analysis confirmed the presence of transcripts for variant 1 of the echinoderm microtubule-associated-like protein-4 gene (*EML4*) –*ALK* fusion gene. The patient received one cycle of chemotherapy with paclitaxel and carboplatin, but treatment was then withdrawn because of disease progression. As a second-line treatment,

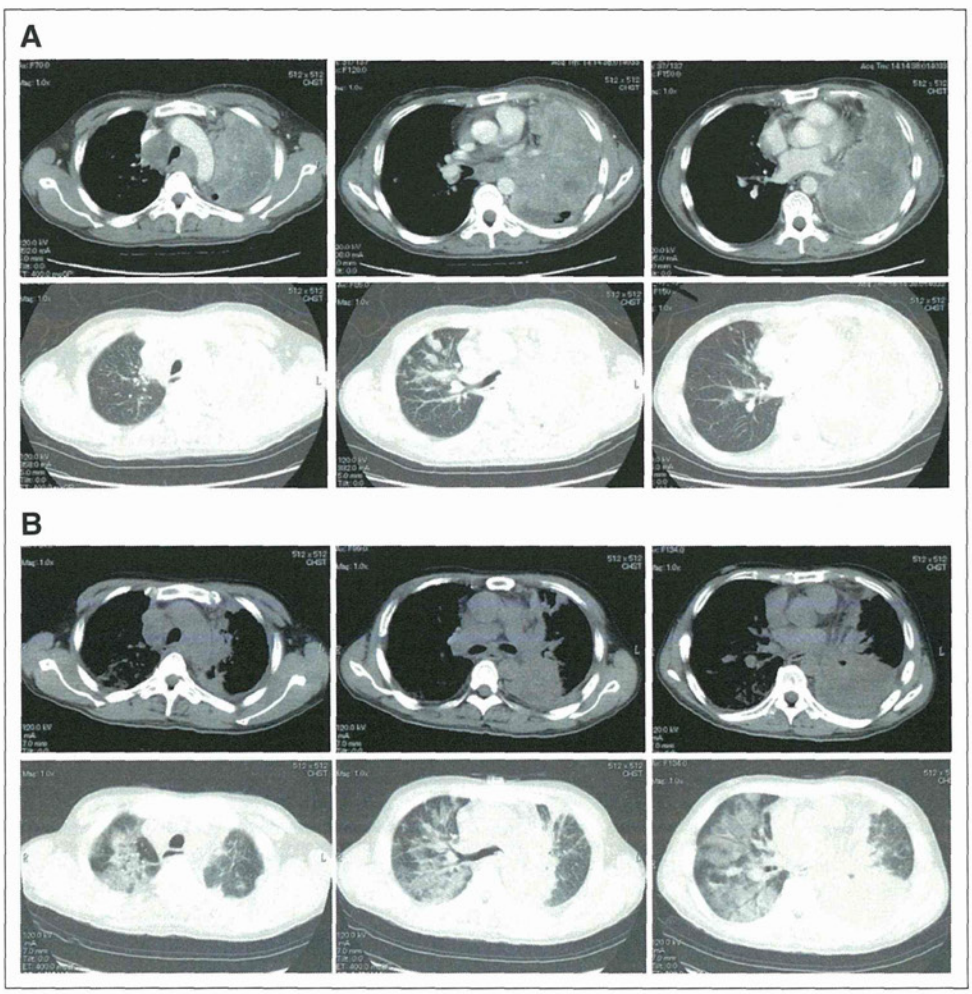

Fig 1.

crizotinib was administered orally at a dose of 250 mg twice daily. After 9 days of crizotinib, the patient developed acutely deteriorating dyspnea without demonstrable infection. With the patient breathing oxygen via a mask at a flow rate of 10 L/min, arterial blood gas determination revealed a P_aO_2 of 61.5 mmHg, a P_aCO_2 of 36.0 mmHg, and a pH of 7.46. A computed tomography scan of the chest showed extensive bilateral ground-glass opacities throughout both lungs, despite obvious shrinkage of the primary tumor lesions in his left lobes (Fig 1A, before crizotinib; Fig 1B, after crizotinib [day 9]). Crizotinib treatment was immediately discontinued, and methylprednisolone pulse therapy (1 g once per day for 3 days) was initiated. Empirical treatment with meropenem, ciprofloxacin hydrochloride, and trimethoprim-sulfamethoxazole was also administered. The patient nevertheless developed acute lung injury in accordance with the Lung Injury Score definitions,[6] and he died 21 days after his first administration of crizotinib. Postmortem analysis of a specimen of the right lung by hematoxylin-eosin (HE) staining revealed juvenile fibroblast hyperplasia (black arrow), nuclear swelling of aberrant alveolar cells (white arrow), and mild infiltration of inflammatory small round cells and neutrophils (Fig 2). The patient was thus diagnosed with diffuse alveolar damage, as previously described for individuals with severe EGFR-TKI–associated ILD.[7,8] No evidence of infection or of other specific etiologies was found. It can be difficult to make a diagnosis of pulmonary toxicity in lung cancer patients because of the high incidence of preexisting lung disease, respiratory tract infections, and progressive malignancy. Despite his smoking history, our patient did not have any preexisting pulmonary fibrosis or chronic obstructive lung disease. He developed rapidly progressive dyspnea with severe hypoxemia and diffuse interstitial infiltrates, which were detected radiographically 9 days after the onset of treatment with crizotinib. The histologic characteristics of his lung tissue were consistent with diffuse alveolar damage, thus opening up the possibility of various potential etiologies. An infectious etiology was ruled out by extensive microbiologic analysis of sputum and blood cultures and by the postmortem examination of the lungs. The pathologic analysis of lung tissue did not reveal any lymphangitic spread of the cancer. The patient's history and clinical examination did not provide any evidence of a toxic origin, prior radiotherapy, collagen vascular disorders, or other usual causes of adult respiratory distress syndrome. The exclusion of these other causes indicated that the severe ILD was most likely attributable to crizotinib treatment. Written informed consent was obtained from the patient's family for publication of this case report and accompanying images.

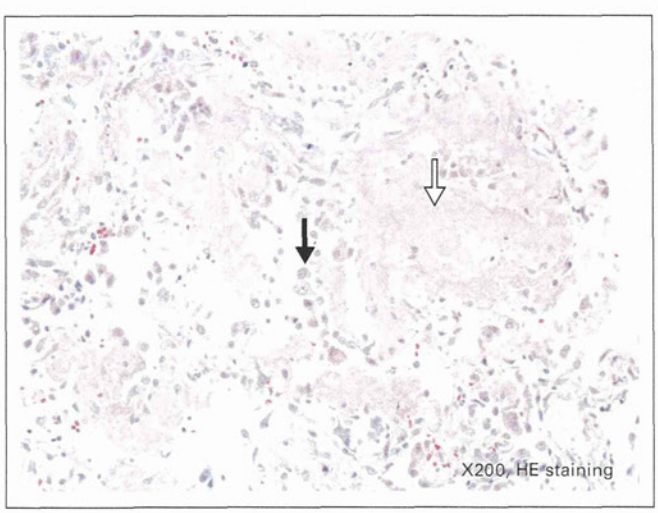

Fig 2.

Discussion

EML4-ALK was recently identified as a transforming fusion gene in NSCLC.[9,10] Preclinical and clinical studies have shown that cancer cells harboring *EML4-ALK* are highly sensitive to ALK inhibition.[3,11] Crizotinib is the first clinically available ALK-TKI and competes with ATP for binding to the tyrosine kinase pocket of the enzyme, inhibiting tyrosine phosphorylation of activated ALK at nanomolar concentrations. On the basis of its pronounced clinical activity and tolerability profile, crizotinib was approved by the US Food and Drug Administration to treat *ALK* rearrangement–positive NSCLC in August 2011. As far as we are aware, our patient is the first reported example of histologically documented crizotinib-associated ILD. Although crizotinib is generally well tolerated, physicians should thus be aware of the possibility of such a severe adverse reaction and full informed consent for treatment should be obtained. We have previously identified male sex, a history of smoking, and coincidence of interstitial pneumonia as independent risk factors for EGFR-TKI–associated ILD[12]; however, it remains unclear whether these risk factors also apply to crizotinib-associated ILD. Given that drug-induced ILD has a high associated mortality, a systematic survey allowing direct determination of the prevalence of and identification of risk factors for crizotinib-induced ILD is warranted.

Akihiro Tamiya
Kinki-Chuo Chest Medical Center, Osaka, Japan

Isamu Okamoto and Masaki Miyazaki
Kinki University, Osaka, Japan

Shigeki Shimizu and Masanori Kitaichi
Kinki-Chuo Chest Medical Center, Osaka, Japan

Kazuhiko Nakagawa
Kinki University, Osaka, Japan

ACKNOWLEDGMENT

The patient described in this report was treated in a crizotinib clinical trial (A8081007, NCT00932893) that was sponsored by Pfizer.

AUTHORS' DISCLOSURES OF POTENTIAL CONFLICTS OF INTEREST

The author(s) indicated no potential conflicts of interest.

REFERENCES

1. Maemondo M, Inoue A, Kobayashi K, et al: Gefitinib or chemotherapy for non-small-cell lung cancer with mutated EGFR. N Engl J Med 362:2380-2388, 2010

2. Mitsudomi T, Morita S, Yatabe Y, et al: Gefitinib versus cisplatin plus docetaxel in patients with non-small-cell lung cancer harbouring mutations of the epidermal growth factor receptor (WJTOG3405): An open label, randomised phase 3 trial. Lancet Oncol 11:121-128, 2010

3. Kwak EL, Bang YJ, Camidge DR, et al: Anaplastic lymphoma kinase inhibition in non-small-cell lung cancer. N Engl J Med 363:1693-1703, 2010

4. Kudoh S, Kato H, Nishiwaki Y, et al: Interstitial lung disease in Japanese patients with lung cancer: A cohort and nested case-control study. Am J Respir Crit Care Med 177:1348-1357, 2008

5. Cohen MH, Williams GA, Sridhara R, et al: FDA drug approval summary: Gefitinib (ZD1839) (Iressa) tablets. Oncologist 8:303-306, 2003

6. Bernard GR, Artigas A, Brigham KL, et al: Report of the American-European consensus conference on ARDS: Definitions, mechanisms, relevant outcomes and clinical trial coordination—The Consensus Committee. Intensive Care Med 20:225-232, 1994

7. Okamoto I, Fujii K, Matsumoto M, et al: Diffuse alveolar damage after ZD1839 therapy in a patient with non-small cell lung cancer. Lung Cancer 40:339-342, 2003

8. Inoue A, Saijo Y, Maemondo M, et al: Severe acute interstitial pneumonia and gefitinib. Lancet 361:137-139, 2003

9. Soda M, Choi YL, Enomoto M, et al: Identification of the transforming EML4- ALK fusion gene in non-small-cell lung cancer. Nature 448:561-566, 2007

10. Soda M, Takada S, Takeuchi K, et al: A mouse model for EML4-ALK-positive lung cancer. Proc Natl Acad Sci U S A 105:19893-19897, 2008

11. Takezawa K, Okamoto I, Nishio K, et al: Role of ERK-BIM and STAT3-survivin signaling pathways in ALK inhibitor-induced apoptosis in EML4-ALK-positive lung cancer. Clin Cancer Res 17:2140-2148, 2011

12. Ando M, Okamoto I, Yamamoto N, et al: Predictive factors for interstitial lung disease, antitumor response, and survival in non-small-cell lung cancer patients treated with gefitinib. J Clin Oncol 24:2549-2556, 2006

DOI: 10.1200/JCO.2012.43.3730; published online ahead of print at www.jco.org on November 19, 2012

